

Collaborative Virtual Screening Identifies a 2-Aryl-4-aminoquinazoline Series with Efficacy in an *In Vivo* Model of *Trypanosoma cruzi* Infection

Taisuke Tawaraishi, Atsuko Ochida, Yuichiro Akao, Sachiko Itono, Masahiro Kamaura, Thamina Akther, Mitsuyuki Shimada, Stacie Canan, Sanjoy Chowdhury, Yafeng Cao, Kevin Condroski, Ola Engkvist, Amanda Francisco, Sunil Ghosh, Rina Kaki, John M. Kelly, Chiaki Kimura, Thierry Kogej, Kazuya Nagaoka, Akira Naito, Garry Pairaudeau, Constantin Radu, Ieuan Roberts, David Shum, Nao-aki Watanabe, Huanxu Xie, Shuji Yonezawa, Osamu Yoshida, Ryu Yoshida, Charles Mowbray, and Benjamin Perry*



Cite This: *J. Med. Chem.* 2023, 66, 1221–1238



Read Online

ACCESS |



Metrics & More

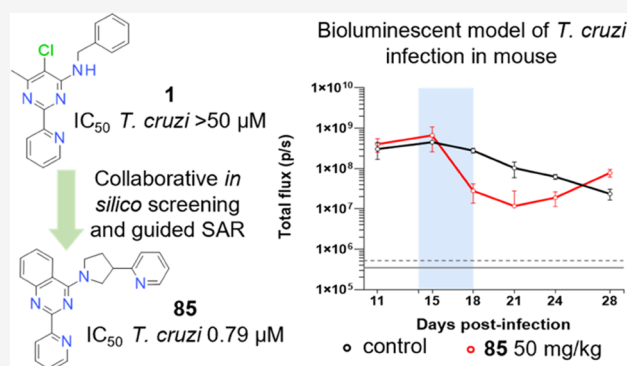


Article Recommendations



Supporting Information

ABSTRACT: Probing multiple proprietary pharmaceutical libraries in parallel via virtual screening allowed rapid expansion of the structure–activity relationship (SAR) around hit compounds with moderate efficacy against *Trypanosoma cruzi*, the causative agent of Chagas Disease. A potency-improving scaffold hop, followed by elaboration of the SAR via design guided by the output of the phenotypic virtual screening efforts, identified two promising hit compounds **54** and **85**, which were profiled further in pharmacokinetic studies and in an *in vivo* model of *T. cruzi* infection. Compound **85** demonstrated clear reduction of parasitemia in the *in vivo* setting, confirming the interest in this series of 2-(pyridin-2-yl)quinazolines as potential anti-trypanosome treatments.



INTRODUCTION

Chagas Disease (CD), classified as a neglected tropical disease (NTD) by the World Health Organization, is caused by an infection of the protozoan kinetoplastid parasite *Trypanosoma cruzi* and demonstrates a broad range in severity including significant morbidity and mortality.^{1–3} In addition to the high incidence of CD in Brazil and Latin America, prevalence is growing in Central America, southern United States, and elsewhere in the world.^{4–12} It is assumed that more than 6 million people are currently infected with this parasite, and over 10,000 deaths per year can be attributed to this disease.^{13,14} Transmission occurs via an insect of the family Reduviidae, trivially known as the “kissing bug”, through the feces of the insect during its blood meal to humans.^{15–17} In the human host, *T. cruzi* parasites can multiply in different cell types, as either the dominant, noninvasive, replicative intracellular amastigote form or as the blood-stage invasive, nonreplicative, trypomastigotes.¹⁸ There is substantial evidence that post-initial infection, the parasites are widespread in the human host, invading many different organs within the body. As detailed in the life cycle of this parasite reported by Centers for Disease Control and Progression (CDC),^{19,20} the disease has two stages: an acute stage and a chronic stage; in the acute stage, most infected adults

demonstrate only mild symptoms; however, this acute phase demonstrates a significantly higher fatality rate among children, currently approximated at around 5%.²⁰ Following the subsidence of the acute phase, the infection then enters a chronic stage, where the parasite remains dormant for many years or even decades in around 70% of infected individuals. Approximately 30% of patients hosting this chronic infection eventually develop symptoms such as chronic heart disease, megacolon/megaesophagus, or both. Oftentimes, the underlying causative chronic *T. cruzi* infection is only detectable when the patient is critically ill or even dead.¹⁰

Despite the prevalence and mortality rate of CD, pharmacological responses for this disease are still not fit for purpose. There is no available vaccine and the current standard drugs, benznidazole and nifurtimox, demonstrate efficacy only in acute infections, where disease diagnosis is rare.^{21–25} Pharmacological

Received: May 17, 2022

Published: January 6, 2023



efficacy of these treatments in chronically infected subjects is less dependable, and suffers from serious side effect profile.^{13,26,27}

Recently, development of a novel class of molecules for CD, CYP51 inhibitors (Posaconazole and E1224, the prodrug of ravuconazole), successfully progressed into clinical development. However, this class of molecules proved to be insufficiently effective in humans, with prevalent treatment failure in patients. General consensus in the scientific Chagas community stresses the need to avoid further development of compounds acting predominantly via this mechanism of action.²⁸ The subsequent attrition of this class of molecules has resulted in a relatively bare R&D pipeline for CD.^{24,25,29–32} There is a critical urgency for development of new treatment options for this disease, which concerns millions of the world's poorest people, particularly in low-to-middle income countries (LMIC) across Latin America. Despite many interesting and fruitful approaches to identify new chemical entities for the treatment of *T. cruzi* infection in the past decade,^{33–40} further research is still required to address CD, with the clear goal of obtaining an effective, orally bioavailable, affordable, and safe molecule effective in both the acute and chronic phases of the disease.

RESULTS AND DISCUSSION

Screening and Initial Hit Identification. Since 2012, one of our organizations (DNDi) has tested over 2 million compounds in high-throughput high-content screening against kinetoplastid parasites including *Leishmania donovani* and *Trypanosoma cruzi*, the causative agents of visceral leishmaniasis and CD, respectively, searching for novel and attractive small-molecule starting points for drug discovery campaigns.⁴¹ Seeking to improve the efficiency and throughput of the triaging of results from these phenotypic screening efforts led to the creation of the NTD Drug Discovery Booster, a precompetitive virtual screening model comprising key players from industrial pharmaceutical R&D.^{42,43}

NTD Drug Discovery Booster. As an alternative to a commercial-analogous approach to initial exploration of chemical space around a new high-throughput screening (HTS) hit, the Drug Discovery Booster (“Booster”) engages collaborative, precompetitive *in silico* screening to extrapolate chemical space around a hit,^{44,45} searching across multiple proprietary pharmaceutical company databases, seeking both close analogues to the hit as well as structurally differentiated scaffold-hop compounds based on the ligand pharmacophore. A hit structure (“Seed”) is shared with scientists at each partner pharmaceutical company, *in silico* similarity searches, often proprietary to the partner, are performed probing the proprietary collections of each partner, and up to 100 prospective “similar” molecules per partner are screened against the parasite(s) of interest. The partners are actively encouraged to use their own definition of “ligand-similarity” in an effort to tap into multiple ways of addressing the same overarching question—“what do you have in your library which resembles the “seed”?” This collaborative effort brings a combination of molecules focused on both SAR annotation as well as more general pharmacophore-led exploration. The results of these experimental screens with the providing partners, as well as anonymized sharing of the structure of the most improved molecule from the entire collaborative screening endeavor (“Improved Hit”), allow a second, more refined iteration of *in silico* screening to be performed, again providing ~100 molecules per partner. Repetition of this iterative screening/

sharing process continues until improvements cease to be made, or until SAR around a chemotype emerges.

The use of orthogonal *in silico* techniques and clearly differentiated proprietary libraries maximizes both the richness of the SAR explored around the initial seed phenotype and increases the chances of identifying an interesting change of chemotype with similar or improved antiparasitic activity via scaffold hop.⁴⁶ These newly identified scaffold hops can be subsequently mined using the same Booster approach, thus maximizing the value of the hits coming from HTS.

Hit Identification. 2-Arylpyrimidine **1** (Figure 1) was identified as a potential starting point and anti-kinetoplastid

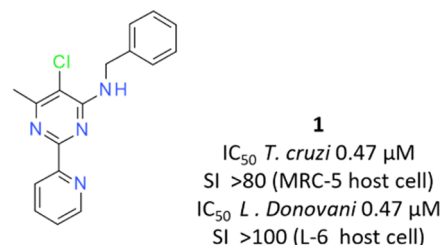


Figure 1. Initial hit compound **1** from high-throughput screening (HTS).

Booster seed based on data from a HTS against both *T. cruzi* and *L. donovani* (the causative agent of visceral leishmaniasis).⁴¹ Compound **1** demonstrated sub-micromolar potency in an intracellular *T. cruzi* infection assay, and an independent batch of **1** demonstrated similar levels of efficacy in an axenic *L. donovani* model (see Supporting Information 1).⁴⁷ Both assays demonstrated a wide selectivity index (SI) between antiparasitic efficacy and cell line cytotoxicity (MRC5 and L-6 cells as controls, respectively). Evaluation of the literature around this 2-arylpyrimidine core revealed extensive general coverage (>25,000 references in scifinder);⁴⁸ however, only one mention of such a chemotype with efficacy in the kinetoplastid field was identified, the mTOR inhibitor NVP-BE235,^{49,50} which despite sharing a 2-arylpyrimidine motif we considered sufficiently structurally differentiated to validate continued evaluation of **1**. Compound **1** did not present any PAINS motif as evaluated by SwissADME;^{51,52} nevertheless, we were cautious about the potential for metal chelation in the 2-(pyridin-2-yl)pyrimidine core leading to false positive or pan-cytotoxicity results. We therefore targeted early evaluation of a compound from the series in an *in vivo* proof of concept (PoC) infection model as a key go/no-go decision point for further work.

Hit Elaboration and Validation via Collaborative *In Silico* Screening. Compound **1** was submitted as a “seed” to the partners of the NTD Booster consortium: AstraZeneca plc, Eisai Co., Ltd., Shionogi & Co., Ltd., Takeda Pharmaceutical Company Ltd., and Celgene Corporation. Since the precompetitive mechanism of the Booster project requires anonymity and a high degree of confidentiality on the *in silico* methods and library composition between partners, identities of the partners are presented as blinded in this study as “Companies A–E”. Four of these companies participated in the first cycle of booster screening, these were joined by the fifth company for the second round of screening, this company having joined the consortium in the interim. An overview of the general Booster process and results are shown in Figure 2.

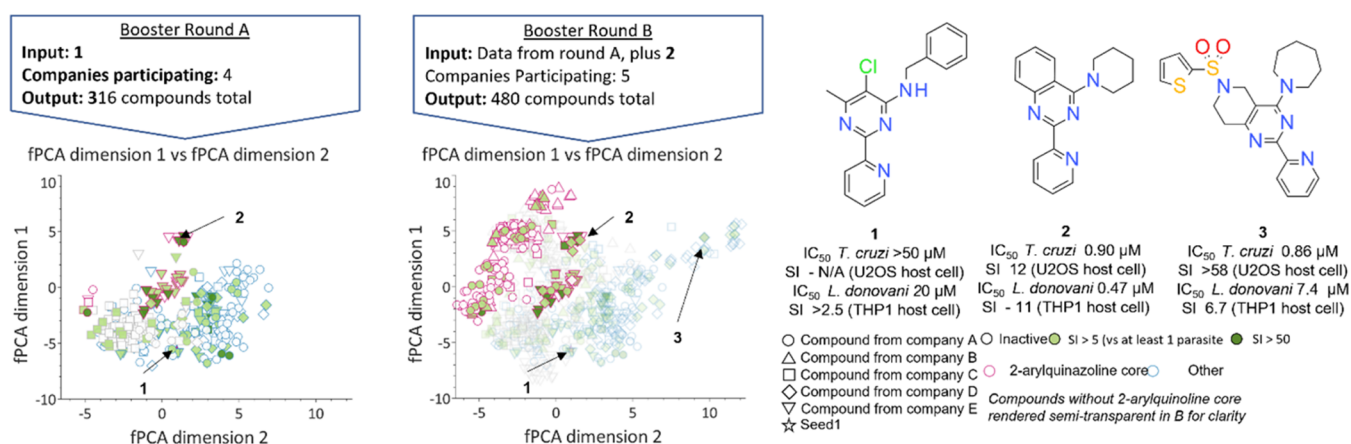


Figure 2. Overview of the booster virtual screening process.

Table 1. Overview of the *In Silico* Approach Taken by Each Partner Company, along with the Number of Compounds Furnished from Each Partner

company and computational approach ^a	total	number of compounds booster round A/B (actives) ^b	
		2-arylpyrimidine ^c	2-arylquinazoline ^d
A—the top scoring 150 compounds were selected by Tanimoto similarity calculation using the FCFP4 fingerprint, followed by refinement to 96 compounds based on maximized diversity	192	22/11 (9)	2/33 (7)
B—similarity search using Daylight ⁵⁹ and Chemaxon ⁶⁰ fingerprints and ROCS ⁶¹ TanimotoCombo scoring	119	27/62 (8)	1/5 (5)
C—ECFP4 similarity (Tanimoto cut-off 0.6) and in-house fingerprint search (Tanimoto cut-off 0.7). Subsequent in-house “quality”, commercial availability, and IP filters	176	83/0 (14)	3/81 (25)
D—series of similarity and substructure-based queries prioritized with Tanimoto similarity calculated by ECFP4	182	53/0 (24)	30/3 (24)
E—ECFP4 similarity (initial Tanimoto cut-off 0.7 descending incrementally until sufficient compounds had been identified)	126	0/3 (1)	0/58 (17)
all companies	795	185/76 (56)	36/180 (78)

^aFurther information is found in Supporting Information 1. ^bActives defined as compounds with SI > 5 against one or both parasites. ^cCompounds with a 2-arylpyrimidine core. ^dCompounds with a 2-arylquinazoline core.

Partners performed ligand-based virtual screening against their proprietary compound collections using the partner-specific *in silico* similarity searches approach as described in Table 1 (see Supporting Information 1 for detailed description). The compounds identified via these virtual screening efforts (316 compounds in total, ~80 compounds per partner) were then investigated in high-content cell-based *T. cruzi* and *L. donovani* infection assays using U2OS and THP1 host cells, respectively [Booster Round A (Figure 2)]. A control sample of 1 was included in both assays. The assay read-outs from these high-content approaches demonstrate a compound's efficacy at total parasite clearance as well as host cell cytotoxicity, yielding an antiparasitic IC_{50} , a host cell CC_{50} , and a selectivity index (SI) between the two read-outs ($SI = \text{host cell } IC_{50} / \text{parasite } IC_{50}$; see the Supporting Information for more details). Compounds with a SI > 5 against either *L. donovani* or *T. cruzi* were considered as demonstrating legitimate antiparasitic activity, and compounds with SI > 50 against either parasite were classified as being of high potency. The results of the virtual screening and experimental parasitology of this selection of compounds displayed as a 2D chemical space representation generated via principal component analysis of chemical fingerprints (fPCA) and calculated physicochemical properties (PCA) are shown in Figure 2 (RDKit nodes in Knime used to generate chemical descriptors, Morgan 1024 Bit fingerprints, and to run principal component analyses). Despite initial hit 1 demonstrating significantly reduced potency in the high-content assays used for the screening of the virtual screen output relative to the

potency seen in the HTS assays via which it had been identified, of the 316 compounds provided, 98 compounds (31%) demonstrated activity, and 18 compounds (6%) were considered highly active. Of the 316 compounds, 58% retained the 2-arylpyrimidine core of the initial seed compound, and the remaining 42% were considered to contain scaffold hops away from the core motif. Within the latter, we identified a small subset of 2-arylquinazolines, exemplified by compound 2, with significant potency against both *T. cruzi* and *L. donovani*. Interestingly, despite the relative ubiquity of quinazolines in the med chem literature, the majority of the 2-arylquinazolines within the screening set (>80%) had been provided by a single Booster partner. Rationalizing that the libraries of the other partners would contain a significant number of 2-arylquinazolines, we repeated the booster *in silico* screening approach with the participating booster companies [Booster Round B (Figure 2)]. For this second cycle, each company received the HTS data from their respective compounds. In addition, the structure and data for 2 was shared with all partners, effectively informing all partners that 2-arylquinazolines were generally more potent than 2-arylpyrimidines. The results of this second round of screening (479 compounds in total) are shown in Figure 2. This second round identified further 180 compounds of 2-arylquinazolines, where 30% were considered as active. In addition, some more highly active compounds provided by partners based on further scaffold hop from the 2-arylquinazoline motif were identified, as exemplified by 3.

Chart 1. Compounds Identified via the Booster Process—Generic Overview of SAR from Booster Only

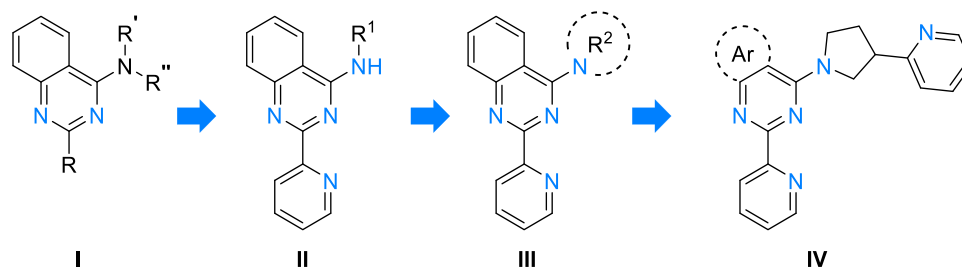
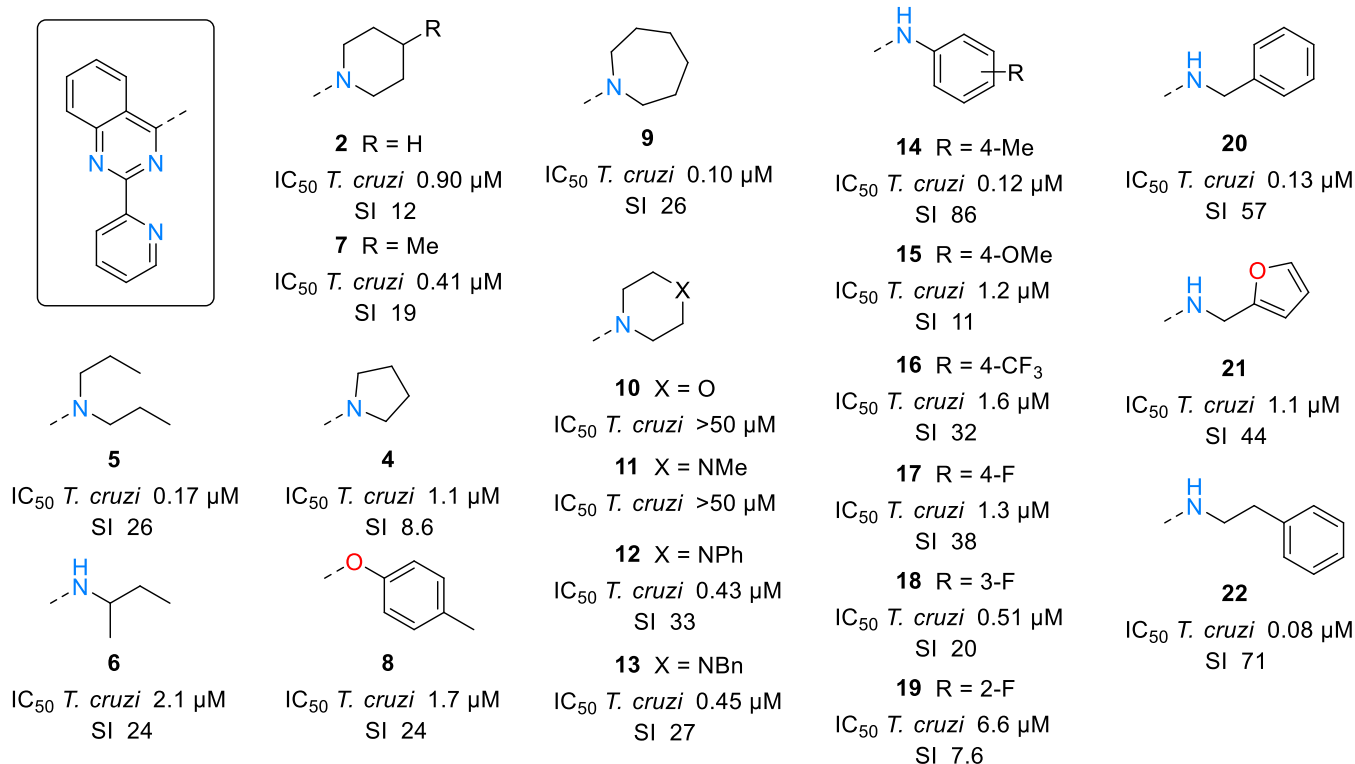
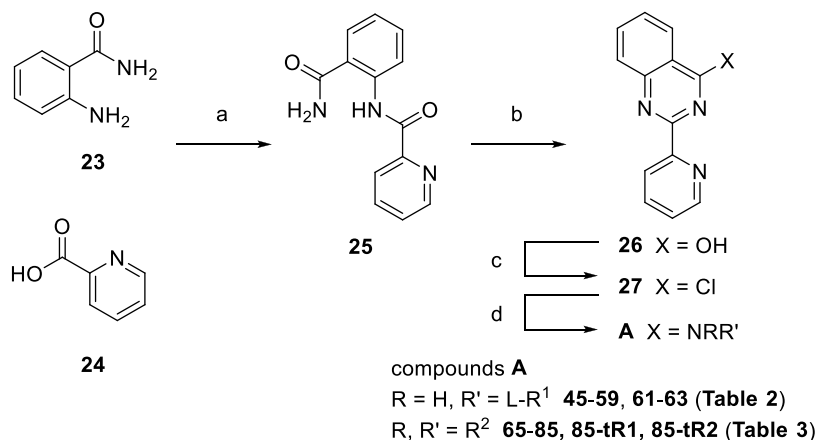


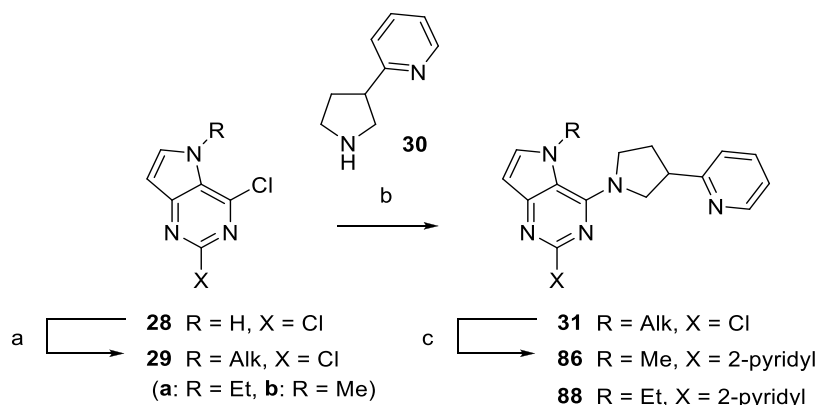
Figure 3. Overview of the post-screening design strategy.

Scheme 1. Synthesis of Intermediate 27 and Analogue Preparation of Quinazoline Derivatives^a

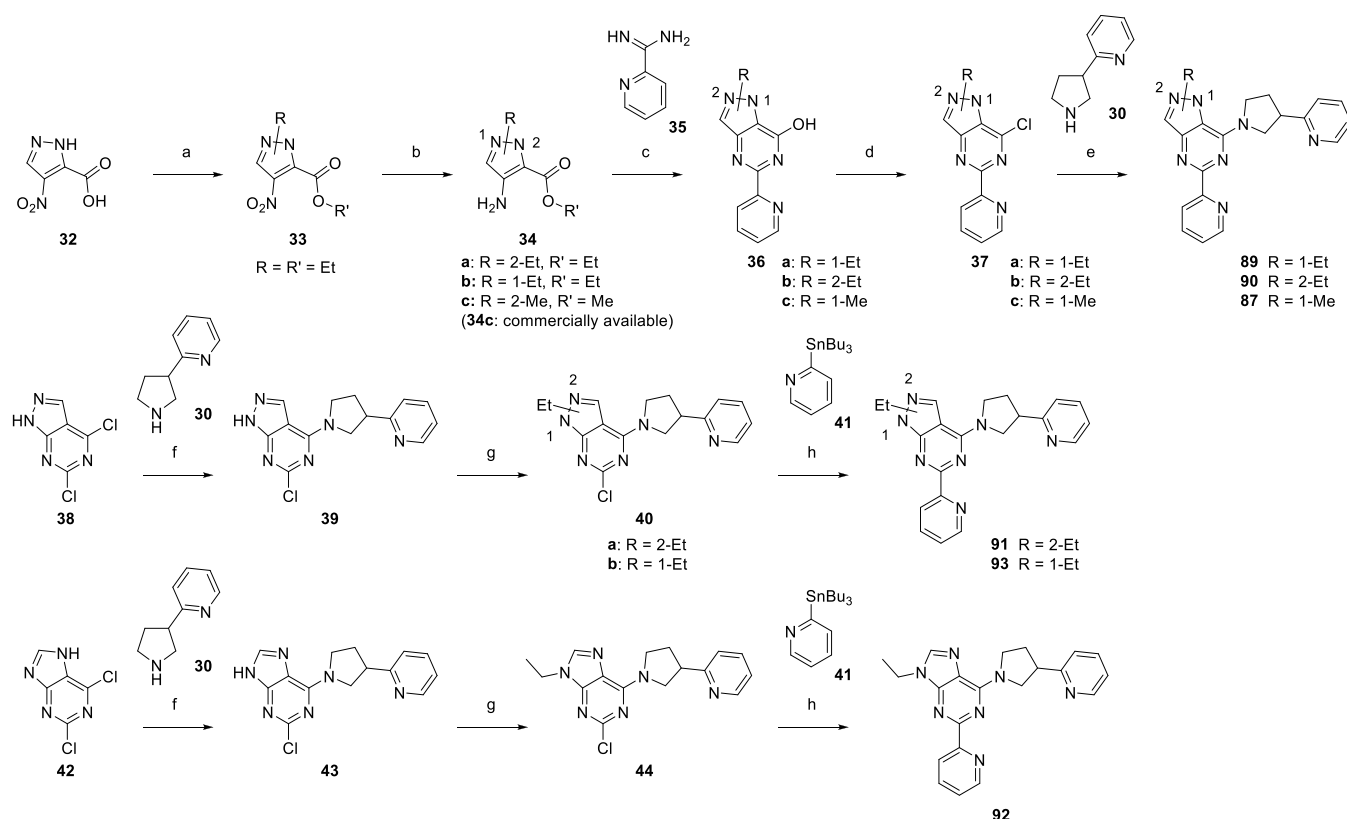
^a Reagents and conditions: (a) HOBT, EDCI, TEA, DMF, rt, 24 h, 85%; (b) 1 N NaOH (aqueous), MeOH, reflux condition, 1 h, 66%; (c) POCl₃, TEA, toluene, reflux condition, overnight, 83%; and (d) amines, *n*-butanol, 50–110 °C, 12–16 h, or DIEA, solvent (MeCN, DMA or NMP), MW 100–170 °C, 0.5–1 h, 3–98%.

Combining the results from these two rounds of collaborative virtual screening allowed us to build a strong picture of the SAR

around this 2-arylquinazoline motif, itself identified as a scaffold hop via the same virtual screen cycle. The general SAR of the

Scheme 2. Core Modification and Analogue Preparation of Pyrrolo[3,2-*d*]pyrimidine Derivatives^a

^aReagents and conditions: (a) alkyl iodides, Cs₂CO₃, DMF, rt, overnight, 70%; (b) 2-(pyrrolidin-3-yl)pyridine (**30**), DIEA, THF, rt, 10 h, 71–77%; and (c) (2-pyridine)cyclic-triylborate lithium salt, Pd₂(dba)₃, cuprous chloride, butyl di-1-adamantylphosphine, potassium *tert*-butoxide, DME, MW 120 °C, 3 h, 19–43%.

Scheme 3. Further Core Modification and Analogue Preparation of Pyrazolopyrimidine and Purine Derivatives^a

^aReagents and conditions: (a) ethyl iodide, K₂CO₃, DMF, rt, 3 h, 70%; (b) iron powder, NH₄Cl, EtOH/H₂O, reflux condition, 2 h, 70%; (c) picolinimidamide (**35**), DIEA, EtOH, reflux condition, 12 h, 50–93%; (d) POCl₃, toluene, reflux condition, 2 h, 58–87%; (e) **30**, *n*-butanol, 100 °C, overnight, or DIEA, MeCN, MW 120 °C, 2 h, 22–75%; (f) **30**, TEA, EtOH, 100 °C, 1 h, or rt, overnight, 27–80%; (g) ethyl iodide, NaH, DMF, rt, 16 h, 37–59%; and (h) 2-(tributylstannyl)pyridine (**41**), Pd(PPh₃)₄, 1,4-dioxane, reflux condition, 16 h, 11–31%.

series informed by compounds 4–22 originating directly from Booster virtual screening (Chart 1) encouraged us to initiate further profiling and analoging, and we instigated a strategy to explore the other substituent positions of quinazoline illustrated by compound designs I–IV (Figure 3).

This strategy entailed variation of (i) the 2-position of quinazoline to understand the importance of the 2-(pyridin-2-yl) motif, (ii) probing the 4-position of the quinazoline core with both acyclic and cyclic amines, (iii) structurally diverse core

scaffold replacements with 6,6- or 5,6-membered aromatic ring. In all cases, we evaluated these changes for both *T. cruzi* activity and pharmacokinetic properties to rapidly identify potential candidates for *in vivo* PoC studies.

Prior to initiating these further studies and to give confidence that the data obtained from the booster virtual screening was correct, we selected four compounds (**4**, **13**, **18**, **20**) from the screening for resynthesis and retest in orthogonal assays. This effort served two purposes—first, to ensure that analytically pure

samples of the compounds coming from the HTS collections of the pharmaceutical companies could be replicated, indirectly qualifying the booster data set and second, to ensure that the activity we were seeing was not confined to a single antiparasitic assay system. The results of this checking process were uniformly positive, with resynthesized batches of the four compounds giving similar levels of potency, which were then reconfirmed in orthogonal antiparasitic assays against *T. cruzi* (MRC5 background cell line) and leishmania infantum (PMM background cell line). Full results from this secondary check are provided in [Supporting Information 1](#).

Synthesis. The synthesis of key intermediate **27** was conducted using readily available starting materials and standard synthetic modifications as shown in [Scheme 1](#).⁵³ Amidation of 2-aminobenzamide (**23**) with pyridine-2-carboxylic acid (**24**) yielded *N*-(2-carbamoylphenyl)pyridine-2-carboxamide (**25**), followed by reaction with methanolic sodium hydroxide heated under reflux condition to afford 2-(pyridin-2-yl)quinazolin-4-ol (**26**). Treating **26** with POCl₃ with TEA yielded 4-chloro-2-(pyridin-2-yl)quinazoline (**27**). Final compounds **A** (**45–59**, **61–63**, **65–85**, **85-tR1**, **85-tR2**) were then prepared from **27** by simple S_NAr transformation with various amines in step (d).

The synthetic routes for core modification to pyrrolo[3,2-*d*]pyrimidine are exemplified in [Scheme 2](#). From the starting material 2,4-dichloro-5*H*-pyrrolo[3,2-*d*]pyrimidine (**28**), we synthesized *N*-alkylated 2,4-dichloro-5*H*-pyrrolo[3,2-*d*]pyrimidines (**29**) by the reaction with alkyl iodides and Cs₂CO₃ in DMF. In the presence of DIEA in THF, 2-(pyrrolidin-3-yl)pyridine (**30**) was reacted with intermediates **29** to afford 2-chloro-5-alkyl-4-(3-(pyridin-2-yl)pyrrolidin-1-yl)-5*H*-pyrrolo[3,2-*d*]pyrimidines (**31**). Carbon–carbon bond formation via the palladium-catalyzed coupling reaction of (2-pyridine)cyclic-triisobutylborate lithium salt with aryl chlorides **31** furnished the desired compounds **86** and **88**.

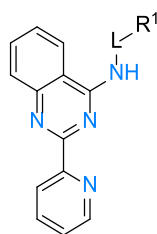
Procedures used to get further core-modified compounds are shown in [Scheme 3](#). Alkylated intermediates **33** were synthesized from commercially available starting material 4-nitro-1*H*-pyrazole-3-carboxylic acid (**32**) in the presence of ethyl iodide and K₂CO₃ in DMF and isolated as a mixture of regioisomers. The reduction of the nitro group of **33** was conducted with iron powder and NH₄Cl in EtOH/H₂O at reflux condition, and two isomers, 1-ethyl and 2-ethylpyrazole intermediates (**34**), were successfully isolated separately. We obtained bicyclic intermediates **36** from **34** and picolinimide (**35**) reacted with DIEA in EtOH under reflux condition. We then obtained chloro-substituted intermediates **37** from **36** by treating with POCl₃ in toluene under reflux condition. Compounds **87**, **89**, and **90** were synthesized by S_NAr transformation from intermediates **37** as described previously. Another two compounds **91** and **93** were prepared in three steps. Intermediate **39** was provided by S_NAr reaction with 4,6-dichloro-1*H*-pyrazolo[3,4-*d*]pyrimidine (**38**) and **30**. An ethyl group was introduced to the main core by treating with ethyl iodide and NaH to get **40**. In the final step, we introduced the 2-pyridyl group by coupling reaction with 2-(tributylstannyl)pyridine (**41**) to afford **91** and **93**. Compound **92** was also synthesized from 2,6-dichloro-9*H*-purine (**42**) using similar conditions for compounds **91** and **93** as described above.

Biological Evaluation. The inhibition of *T. cruzi* in a whole cell parasite assay (amastigote form) was adopted as the primary *in vitro* activity screen (see [Supporting Information 1](#) for further details). Primary physicochemical and ADME evaluation included measurement of log *D* (pH 7.4), kinetic solubility in

phosphate buffer (pH 6.8), *in vitro* microsomal metabolism in mouse and human, and PAMPA permeability (for all compounds see the table in [Supporting Information 2](#)).

Results and Discussion. From the output of the Booster screening, we identified many interesting compounds with diverse profiles as shown in [Chart 1](#). Driven predominantly by two of the booster partners (Takeda, DNDi), but with occasional input and oversight from all other partners in the project, we proceeded toward a classical medicinal chemistry optimization based on these preliminary SAR data. As a first approach to build on the SAR revealed by the Booster screening, replacement of the 2-pyridyl group at 2-position of the quinazoline core with diverse substituents was conducted to better understand the importance of this heterocycle motif on activity (see the table in [Supporting Information 2](#), compounds **SI01–SI10**). A series of compounds were prepared to explore possible substitution of the 2-pyridyl motif, including a “Nitrogen walk” around the pyridyl motif, along with substituted phenyl and other nonpyridyl heteroaryl groups. Unfortunately, all of the modifications away from the 2-pyridyl group resulted in major loss of potency (IC₅₀ > 10 μM) compared to the 2-(pyridin-2-yl)quinazolines identified via the booster screening. These results led us to focus on modification of other parts of the quinazoline core to improve potency based on the initial SAR observations gleaned from surveying the preliminary Booster SAR.

In the second phase of the evaluation strategy, we investigated substituents at the 4-position of the 2-(pyridin-2-yl)quinazoline core, with particular focus on compounds **14** and **20** as interesting starting points for building further SAR. Evaluating the variations of NR'R" groups reported in [Chart 1](#), it was clear that this substituent position is critical for understanding further SAR and enhancing efficacy. At first, the 4-position with differently substituted 4-anilino residues (R¹) was inspected: F, Me, and OMe-substituted compounds **17**, **14**, and **15** gave *T. cruzi* IC₅₀ of 1.3, 0.12, and 1.2 μM, respectively, suggesting that a lipophilic moiety in this position is essential for activity against the parasite ([Table 2](#)). Since aniline structures are known to potentially have cytotoxicity/genotoxicity liabilities, despite being potent, we also decided to replace the benzene ring with a pyridine ring, with the goal of lipophilicity reduction and mitigating toxicity liability. Of the methylated 2- and 3-pyridine derivatives **45–47**, compounds **46** and **47** with 3-pyridyl substitution were less potent, while 2-pyridyl compound **45** retained the *T. cruzi* activity (IC₅₀ 0.10 μM), clearly demonstrating that the pharmacophore is very sensitive to the positioning of heteroatom substituents in this region. This result also validates the possibility to avoid the aniline-type structure at the 4-position of the quinazoline core and that we could adopt other heteroaromatic substitution to maintain the activity. Unfortunately, the low SI value of compound **45** and other compounds in the direct-*N*-aryl substituted series at 4-position remained as an issue. In the interest of reducing planarity and increasing sp³ nature in our molecules, we decided to investigate the increasing linker length between the core quinazoline and the pendant aryl group at 4-position. Interestingly, insertion of a methylene linker between the core and the aryl substituents at the 4-position (**48**, **49**) afforded moderate potency and recovery of SI. Contrary to the findings in the 4-*N*-aryl subset, these extended linker compounds demonstrated greater tolerance for the regioisomeric nature of pyridyl groups, although additional lipophilic shielding of the pyridyl nitrogen (**50**, **51**) demonstrated a trend toward increased potency, further confirming the

Table 2. Inhibitory Activities against *T. cruzi*: Probing the 4-Position with Acyclic Amines

	L	R ¹	<i>T. cruzi</i> ^a IC ₅₀ μM (SI)
14	–	4-Me-Ph	0.12 (86)
15	–	4-MeO-Ph	1.2 (11)
17	–	4-F-Ph	1.3 (38)
45	–	5-Me-pyridin-2-yl	0.10 (<1)
46	–	6-Me-pyridin-3-yl	31 (1.6)
47	–	2,5-Me-pyridin-3-yl	14 (3.6)
48	–CH ₂ –	pyridin-2-yl	4.4 (11)
49	–	pyridin-3-yl	6.3 (8.0)
50	–	3-Me-pyridin-2-yl	1.6 (15)
51	–	6-Me-pyridin-2-yl	2.4 (21)
52	–CH ₂ CH ₂ –	pyridin-2-yl	3.4 (14)
53	–CH(Me)–	–	2.7 (18)
54	–CMe ₂ –	–	1.0 (25)
55	–C(CH ₂ CH ₂)–	–	4.2 (12)
56	–CH ₂ –	1N-Me-pyrazol-4-yl	9.6 (5.2)
57	–	thiazol-2-yl	2.7 (19)
58	–	1N-Me-imidazol-2-yl	3.3 (14)
59	–CH ₂ CH ₂ –	imidazol-1-yl	49 (1.0)
60	–	indazol-5-yl	6.2 (3.5)
61	–	pyrazolo[1,5- <i>a</i>]pyridin-5-yl	11 (2.9)
62	–CH ₂ –	benzoxazol-2-yl	2.5 (16)
63	–CH ₂ CH ₂ –	benzimidazol-1-yl	8.2 (6.1)

^a*T. cruzi* high-content infected cell assay, IC₅₀ of total parasite count; SI = IC₅₀/CC₅₀ against background U2OS cell line.

sensitivity toward lipophilicity/polarity balance in this region of the pharmacophore.

Ethylene-linked 2-pyridyl derivative **52** yielded similar activity to that of methylene linker. When exploring heterocyclic variations of R¹, we observed that thiazole and imidazole derivatives (**57**, **58**) with the methylene linker retained similar potency to the corresponding pyridyl sidechain, while pyrazole and imidazole analogues (**56**, **59**) with methylene or ethylene linker significantly reduced potency relative to compound **48**. These results clearly demonstrated that some variation around the linker is acceptable for this series. We further explored the scope around this methylene linker chain with methyl, dimethyl, and cyclopropyl substitution (**53**, **54**, and **55**). Compared with compound **48**, these changes resulted in maintained or improved potency, with dimethyl-substituted linker compound **54** demonstrating a well-balanced combination of potency and selectivity index.

Only moderate potency was observed by introduction of 6,5- or 5,6-membered bicyclic substituents (**60**–**63**) without any significant improvement of SI over the monocyclic derivatives. This suggested that heteroaromatic-substituted analogues such as pyridine or small heteroaromatic groups, along with an additional linker chain, were the most appropriate option for the 4-position to balance inhibitory activity against *T. cruzi*. Unfortunately, none of these changes resulted in significant

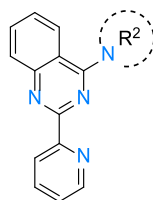
positive impact on metabolic stability, with the exception of compounds **54** and **55** (Table 5). Therefore, we concentrated our efforts elsewhere to find more potent compounds with reasonable SI and improved metabolic stability profiles.

We attempted to replace the NH linker with a series of closed-ring analogues with the aim of retaining the potencies observed for linear analogues while improving the overall physicochemical properties and SI. The hit screening compounds **2** (IC₅₀ 0.90 μM) and **12** (IC₅₀ 0.43 μM) provided the initial inspiration for this strategy. Exploring variations of the R² substituent at 4-position of 2-(pyridin-2-yl)quinazoline core with different heterocyclic rings (piperidine, piperazine, pyrrolidine, and their fused-ring analogues) revealed further SAR trends as depicted in Table 3. Building off compounds **2** and **7**, we designed further piperidine analogues to identify the favorable substitutions around the piperidine ring. As expected from previous SAR observations, we found these lipophilic groups retained high potency, but unfortunately *in vitro* mouse and human clearance remained poor (Table 5). Addition of polar groups such as nitrile at both 3- and 4-positions of the piperidine (**65**, **66**) dramatically reduced both the potency and SI. This data reinforced the view that building in much needed polarity in this area of the molecule would remain challenging. Both 3-phenyl (**67**) and 3-(pyridin-2-yl) (**68**) substitution retained moderate potency as expected, but with some decreased SI. In addition, compound **67** also exhibited poor metabolic stability in both mouse and human. Combination of a phenyl and hydroxy group at 4-position (**69**) as an attempt to building both aromaticity as well as buried polarity in the piperidine subseries unfortunately resulted in reduced potency. A series of fused semisaturated bicyclic analogues **71**–**74** showed weak activities, with the exception of 1,2,3,4-tetrahydroisoquinoline analogue **70**, once again reinforcing the propensity for lipophilicity in this area of the pharmacophore.

Next, we investigated piperazinyl analogues, following up the potency observed in booster-identified compound **12**. In general, across all variations of R², the *in vitro* activity of the piperazinyl compounds was interesting and a similar pattern emerged to the earlier observation that lipophilic phenyl and benzyl group boosted potency (**12**, **13**). From these observations, we observed again that balance of lipophilicity and a certain size of substituent appeared to be required at the R² site.

Following on from the piperazines, we decided to check the impact of reducing the ring size linking R² to the 4-position, since pyrrolidine analogue **4** showed moderate potency. As anticipated by the previously revealed SAR, introduction of polar substituents at 3-position of pyrrolidine, such as carbonitrile, carboxamide, or carboxylic acid (**77**, **78**, and **79**), significantly reduced the potency, while substituted aromatic analogues exemplified by **80**, **81** demonstrated good activity. Unfortunately, these modifications did not result in improved metabolic stability. A more polar 3-hydroxy analogue of **80** (**82**) reduced the potency, while addition of fluorine into the phenyl ring of **80** (**83**) retained potency but failed to stabilize the metabolic profile as well. Introduction of nitrogen into the phenyl ring (**85**) to reduce log *D* and in turn improve metabolic stability showed well-balanced profiles of potency and metabolic stability along with better solubility in comparison with phenyl analogue **80** (Table 5). The position of pyridine substitution on pyrrolidine was investigated, with the 3-position of pyrrolidine proving more beneficial (**85**). Thus, 3-(pyridin-2-yl)pyrrolidine analogue **85** provided a good balance between potency and

Table 3. Inhibitory Activities against *T. cruzi*: Probing the 4-Position with Cyclic Amines



	R ²	R or X, Y	<i>T. cruzi</i> ^a IC ₅₀ μM (SI)	
2		H	0.90 (12)	
7		4-Me	0.41 (19)	
64		3-Me	0.43 (19)	
65		3-CN	18 (2.7)	
66		4-CN	24 (2.1)	
67		3-Ph	0.36 (6.4)	
68		3-(pyridin-2-yl)	1.3 (7.3)	
69		4-Ph, 4-OH	3.3 (15)	
70			X, Y = CH	0.72 (6.6)
71	X=CH, Y=N		7.4 (4.9)	
72	X=N, Y=CH		9.2 (5.5)	
73			27 (1.9)	
74			21 (2.3)	
12		Ph	0.43 (33)	
75		pyridin-2-yl	3.3 (6.4)	
76		6-Me-pyridin-2-yl	1.9 (7.0)	
4		H	1.1 (8.6)	
77		3-CN	7.0 (7.2)	
78		3-CONH ₂	23 (2.2)	
79		3-CO ₂ H	> 50	
80		3-Ph	0.28 (9.7)	
81		3-OPh	0.36 (6.5)	
82		3-Ph, 3-OH	3.5 (2.8)	
83		3-(4-F-Ph)	0.41 (9.2)	
84		2-(pyridin-2-yl)	1.8 (25)	
85		3-(pyridin-2-yl)		0.79 (9.1)
85-tR1 ^b				1.1 (4.2)
85-tR2 ^b			0.96 (6.4)	

^a*T. cruzi* high-content infected cell assay, IC₅₀ of total parasite count; SI = IC₅₀/CC₅₀ against background U2OS cell line. ^bChiral enantiomer.

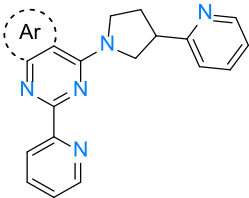
lipophilicity. The component enantiomers of compound **85** were prepared from enantiopure building blocks (see Support-

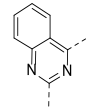
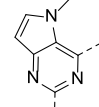
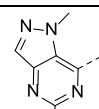
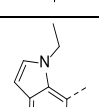
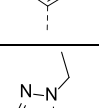
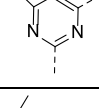
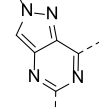
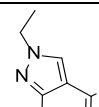
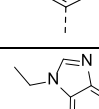
ing Information 1) and both enantiomers **85-tR1** and **85-tR2** were found to be equipotent against *T. cruzi*, demonstrating IC₅₀ values in line with those of racemic **85**. Therefore, further evaluation of **85** proceeded as the racemate. Following this expansion of the SAR, we concluded that, in general, piperidine (compounds **7**, **64**, **67**, **68**) and piperazine (compounds **12**, **76**) analogues were moderate in potency, whereas pyrrolidine analogues (compounds **80**, **81**, **83**, **85**) retained the expected higher potency level, possibly due to the favorable introduction of aromatic rings.

To confirm that the series was not exerting an antiparasitic effect via an inhibition of TcCYP51, we tested one of the most potent analogues, compound **83** (0.41 μM), in a direct TcCYP51 inhibitory assay.^{28,54} Compound **83** demonstrated no inhibitory activity against TcCYP51 at concentration up to and including 100 μM, confirming that this chemical series does not exhibit its trypanocidal effect via a CYP51-mediated pathway. The physicochemical and *in vitro* DMPK profiles for selected compounds from the overall SAR studies were evaluated to identify compounds, which could be progressed to the critical *in vivo* PoC studies. In Table 5, the summary of the *in vitro* mouse and human microsomal metabolism, solubility at pH 6.8, and permeability are presented. Reviewing both these data and *in vitro* potency (IC₅₀ and SI), we noted compounds **54** and **85** were the molecules with greatest potential for further investigation. Mouse and human microsomal CL_{int} for compound **85** clearly demonstrated only moderate *in vitro* clearance, whereas for compound **54**, unfortunately, the microsomal CL_{int} was not determined due to difficulties with the chromatographic analysis in our assay system. However, both the mouse and human microsomal metabolism of cyclopropyl analogue **55** showed low clearance, suggesting that compound **54** also has good metabolic stability. Both compounds **54** and **85** displayed acceptable kinetic solubility at pH 6.8 (**83**, **83** μg/mL, respectively). Plasma protein binding measured in mouse species for compound **54** was reported with 94.2%, whereas that for compound **85** with 99.9%. We hypothesized that this significant difference in plasma protein binding was likely to have some impact on the PK study, and both compounds **54** and **85** were worthy of simultaneous progression to maximize understanding of any efficacy observed in *in vivo* infection models.

Based on the initial SAR findings, we hypothesized that the higher log *D* of the quinazolinone core compounds explored to that point had a negative impact on overall physicochemical and ADME properties for this series. From the lead identification study as described above, compounds **54** and **85** were identified as the most interesting compounds so we decided to target further optimization of lipophilicity by reducing the log *D* values of the core heterocycle. We initiated a scaffold hop with different variations of heterocyclic core as demonstrated by **86**–**93** in Table 4. *N*-Alkylated pyrrolopyrimidine-type core compounds **86** and **88** maintained or enhanced potency up to 4-fold along with reduction of log *D* by 0.5–0.8 units in comparison with compound **85**. But unfortunately, both compounds demonstrated an issue linked to chemical stability when attempting to determine *in vitro* metabolic profiles, and further investigation of these compounds was therefore not pursued. Other exploratory core shifts with pyrazolopyrimidine and purine ring (**87**, **89**–**93**) raised concerns for low SI values and were not pursued further (Table 5).

Finally, in addition to these scaffold-hop attempts, we decided to return once more and revisit the importance of the pyridin-2-

Table 4. Inhibitory Activities against *T. cruzi*: Investigation of Core Changes


	Bicyclic core	<i>T. cruzi</i> ^a IC ₅₀ μM (SI)
85		0.79 (9.1)
86		0.56 (16)
87		1.8 (2.9)
88		0.18 (28)
89		1.2 (2.7)
90		0.10 (2.8)
91		1.5 (2.3)
92		2.7 (2.7)
93		18 (2.8)

^a*T. cruzi* high-content infected cell assay, IC₅₀ of total parasite count; SI = IC₅₀/CC₅₀ against background U2OS cell line.

Table 5. *In Vitro* ADME Properties of Some Analogues^a

compound	Cl _{int} microsomes (μL/min/mg) mouse/human	solubility pH 6.8 (μg/mL)	PAMPA pH 7.4 (nm/s)
7	>500/112	59	441
12	>500/95	15	291
47	154/<1	31	201
54	ND	83	258
55	24/7	84	219
64	452/188	69	364
67	318/205	0.1	416
70	464/150	10	408
80	>500/NT	0.7	NT
81	>500/361	7.7	430
83	>500/NT	NT	NT
85	258/73	83	319
86	ND	90	219
87	ND	99	171
90	70/<1	94	220

^aND: not determined, NT: not tested.

yl group in the 2-position of the core quinazoline, while retaining the 3-(pyridin-2-yl)pyrrolidine motif of **85** at the 4-position. Once again, these studies revealed that the 2-pyridyl motif remained essential to achieve both potency and acceptable SI against background cell cytotoxicity (see the table in [Supporting Information 2](#), compounds **SI11–SI26**).

Initial PK and Tolerability Assessment. After evaluating all other profiles, compounds **54** and **85** were selected for further evaluation to ratify the PoC in a rodent model of acute *T. cruzi* infection. Compound **54** was dosed intravenously (i.v.) and orally (p.o.) to female Balb/c mice at 1 and 50 mg/kg, respectively. Blood concentration–time profiles after oral dosing gave an AUC 59859 ng·h/mL, with **54** demonstrating excellent oral bioavailability (full PK in [Supporting Information 1](#)). No adverse reactions or compound-related side effects were observed following oral administration of this compound at this single dose level, and the compound was progressed for evaluation in a multiday dosing tolerability regimen in healthy mice in which **54** was administered BID orally over 5 days at 10, 50, and 100 mg/kg (1 animal per group). Unfortunately, this preliminary tolerability study ruled out further work with this compound due to abnormal observations in animals at 2 days (100 mg/kg) and 3 days (50 mg/kg) post first dose. These abnormal events included animals being cold to touch, with hunched posture and abnormal gait, as well as decreased activity. To find out potential causes of this toxicity, we investigated off-target selectivity for compound **54** against a panel of 300 kinases (1 μM test concentration) and across a panel of 35 known-liability targets including GPCRs and ion channels in both agonist and antagonist read-out and biochemical functional assay for nuclear hormone receptors and phosphodiesterases (10 μM test concentration). Compound **54** was shown to have no known off-target activity with the exception of 5HT-1A antagonism; however, this was ruled out as the cause of these adverse events due to reports indicating that hypothermia can be elicited by the selective agonism of 5HT-1A in rodent species, whereas antagonists are known to suppress or reverse this agonist-induced hypothermia.⁵⁵ No clear correlation of toxicity was observed, so we decided to deprioritize further off-target toxicity exploration of this compound; however, one ongoing speculation was that this tolerability issue could be linked to a

combination of the high brain penetration profile and moderate free fraction ($B/P > 1$, Table 6). We therefore decided to discontinue any further profiling of compound **54**.

Table 6. Pharmacokinetic and Pharmacodynamic Study in Mice after Intravenous and Oral Administration of **54 and **85****

PK parameters	54	85	85 + ABT^a
i.v. dose (mg/kg)	1	0.1 ^b	2
p.o. dose (mg/kg)	50	50	12.5
C_{\max} (ng/mL)	6237	3363	4243
$AUC_{0-\text{last}}$ (ng·h/mL)	59 859	9607	26 912
plasma CL (mL/min/kg)	12.4	38.5	4.9
plasma V_{ss} (L/kg)	0.909	0.77	0.94
half-life, i.v./p.o. (h)	1.13/ND	−/7.2	1/3.3
oral bioavailability (%)	>100	50	67
brain to plasma ratio	1.6 (0.5 h)	1.66 (1 h)	ND
tolerability (single p.o. dose)	ok	ok	poor
tolerability (5 days BID p.o.)	poor	ok	ND

^a50 mg/kg 1-aminobenzotriazole administered p.o. 2 h prior to i.v. or p.o. dose. ^bAs part of a five-compound cassette PK study.

We proceeded with pharmacokinetic evaluation of compound **85**, which was dosed intravenously and orally to female Balb/c mice at 2 and 12.5 mg/kg, respectively ($n = 3$ mice/dose route) with same dose formulation described for compound **54**, in the presence of 1-aminobenzotriazole (ABT) as a Cytochrome P450 metabolism inhibitor in an effort to boost exposure levels.⁵⁶ Blood concentration–time profiles following i.v. and oral dosing are shown in Supporting Information 1. Compound **85** demonstrated good oral bioavailability in the presence of ABT; however, at this dose, adverse tolerability events were observed after the single dose, manifesting in similar observations to those seen upon multiday dosing with **54**. Compound **85** also demonstrated good oral bioavailability and a moderate-to-high clearance when dosed orally without ABT (0.1 and 50 mg/kg p.o., respectively). Comparing these studies with and without ABT, we concluded that clearance of **85** was likely driven primarily by Cytochrome P450s; however, the bioavailability of **85** when dosed alone was sufficient to merit further investigation. Importantly, no adverse issues were noted during the study in the absence of ABT, so **85** was progressed to a multiday dosing tolerability test. For tolerability test, four female mice were randomly allocated to four groups of one animal/group and administrated with vehicle (0.5% (w/v) HPMC/0.5% (v/v) benzyl alcohol/0.4% (v/v) Tween 80 in purified water) and compound **85** (10, 50, and 100 mg/kg/dose (BID)) for 5 days. As opposed to the findings with **54**, there were no treatment-related mortality, clinical observations, body weight and weight gain, food consumption, and gross pathology at ≤ 100 mg/kg/dose (BID) for **85**. This result demonstrated that, contrary to compound **54**, compound **85** administered by oral gavage to twice per day to female mice for 5 days was well tolerated. Based on these data, the no-observed-adverse-effect-level (NOAEL) was considered to be at 100 mg/kg/dose (BID). Compared with the properties of compound **54**, the desired pharmacokinetic profile of **85** including plasma levels, extended exposure over the dosing interval, and exposure relative to the *in vitro* IC_{50} was not quite as attractive as **54**, mainly linked to the high plasma protein binding observed for **85**. From the previous analysis, compound **85** exhibited a more rapid clearance and had lower plasma concentrations at 24 h, high volume of distribution, long half-life, and high oral bioavailability

compared to compound **54**. However, the improved tolerability profile of **85** suggested this molecule would provide the best preference for PoC.

In Vivo Efficacy Study. The PoC study employed the bioluminescent *T. cruzi* CL Brenner strain described previously by Kelly et al.^{57,58} In this model, parasite burden can be tracked quantifiably *in vivo* via the tissue-penetrating *T. cruzi* strain expressing a novel luciferase that emits tissue-penetrating orange-red light. Five-day BID treatment of mice with acute *T. cruzi* infection with 50 mg/kg **85** from day 14 post-infection reduced the parasite burden by $89.9 \pm 5.1\%$ compared with untreated controls by day 18 post infection (Figure 4).

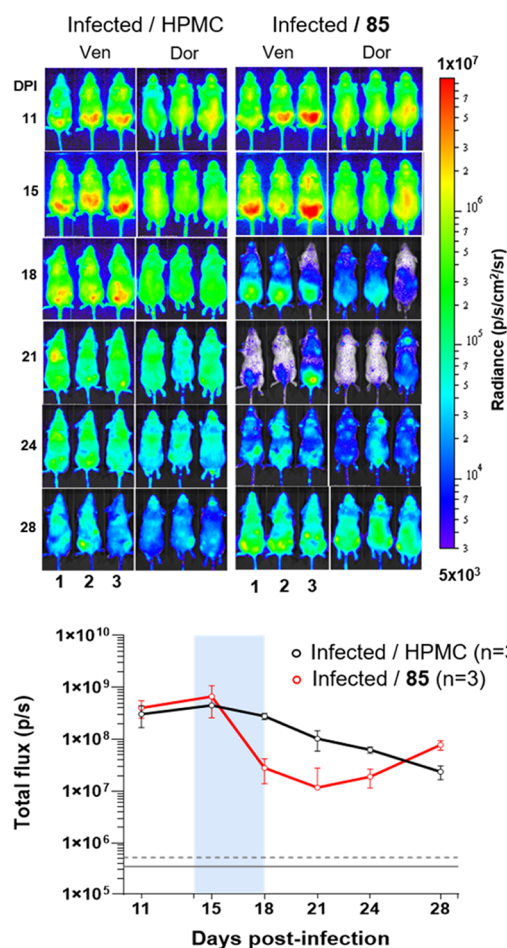


Figure 4. Assessment of compound **85** as a treatment for acute-stage *Trypanosoma cruzi* infections. BALB/c mice ($n = 3$) at the acute stage of infection (14 days) were treated (50 mg/kg, orally, twice daily) for 5 days. The inset graph shows the total body bioluminescence (sum of ventral and dorsal images) of treated (red) and nontreated (black) mice. The blue bar indicates the treatment period. Gray dotted line represents background + SD.

Importantly, in line with the pre-PoC tolerability study in healthy mice, no adverse effects were observed during the treatment duration. While the illustration of efficacy in this *in vivo* PoC study is encouraging and clearly demonstrates that the chemical series antiparasitic effect translates from *in vitro* to *in vivo* efficacy, the overall effectiveness of **85** *in vivo* was considered transient. Even if “cure” was not accomplished with compound **85** in this mouse/parasite combination, as the reduction in parasite burden was not maintained by day 28, the level of efficacy demonstrated in such a stringent test of *in vivo*

efficacy was encouraging and follow-up compounds are being considered for further evaluation.

CONCLUSIONS

The unique NTD Booster approach consisting of DNDi and pharmaceutical R&D enabled the identification of potent and promising 2-aryl-4-aminoquinazoline derivatives by collaborative *in silico* screening. A detailed SAR exploration was conducted around the antiparasitic efficacy of a series of 2-(pyridin-2-yl)quinazolines against *T. cruzi*, and two potential lead compounds **54** and **85** with moderate *in vitro* potency for use in a PoC study were identified. In the case of compound **54**, despite good *in vitro* efficacy and attractive PK, the 5-day tolerability test in noninfected mice failed, with adverse issues such as hypothermia/death. Despite investigation, no proven correlation for this rapid-onset toxicity of compounds **54** was identified, and we decided to stop any further exploration of compound **54**. We hypothesize that these observed toxicity issues could be driven by the as yet unidentified off-target mechanism linked to brain exposure or by higher free plasma fraction relative to compound **85**, which did not demonstrate any adverse events. Compound **85** showed an acceptable range of *in vitro* potency, excellent bioavailability, and acceptable exposure during PK and passed the 5-day tolerability test in healthy animals without any adverse events noted. Compound **85** demonstrated clear, but moderate, activity in an *in vivo* mouse model of acute *T. cruzi* infection. Despite this encouraging result, there remain some key concerns to be solved for this chemotype, particularly around *in vitro* and *in vivo* toxicity profiles and the continued apparent reliance on a bivalent chelation motif in the SAR. Further exploration of this series is ongoing.

EXPERIMENTAL SECTION

General Information and Synthetic Methods. Reactions were run using available starting materials and solvents without further purification. Abbreviations of solvents and reagents are used as follows: CDCl₃, deuterated chloroform; DCM, dichloromethane; DME, 1,2-dimethoxyethane; DMA, *N,N*-dimethylacetamide; DMF, *N,N*-dimethylformamide; DMSO-*d*₆, deuterated dimethyl sulfoxide; EtOAc, ethyl acetate; EtOH, ethanol; H₂O, water; MeCN, acetonitrile; MeOH, methanol; NMP, *N*-methyl-2-pyrrolidone; THF, tetrahydrofuran; DIEA, diisopropylethylamine; EDCI, 1-ethyl-3-(3-dimethylaminopropyl)carbodiimide; HOBT, 1-hydroxybenzotriazole; NH₄Cl, ammonium chloride; Pd₂(dba)₃, tris(dibenzylideneacetone)-dipalladium(0); Pd(PPh₃)₄, tetrakis(triphenylphosphine)-palladium(0); TEA, triethylamine; Cs₂CO₃, cesium carbonate; K₂CO₃, potassium carbonate; MgSO₄, magnesium sulfate; NaH, sodium hydride; NaHCO₃, sodium hydrogen carbonate; NaOH, sodium hydroxide; Na₂SO₄, sodium sulfate; POCl₃, phosphorus oxychloride. Abbreviations of proton nuclear magnetic resonance (¹H NMR) are used as follows: s = singlet, d = doublet, t = triplet, q = quartet, bs = broad singlet, m = multiplet, dd = doublet of doublets, dt = doublet of triplets, tt = triplet of triplets.

Compounds **2–22**, **60**, and **64** were derived from Booster screening compounds and extracted via cherry picking from pharmaceutical company HTS screening collections. Therefore, no spectrum data nor purity data are available beyond reliance on internal company quality controls on their screening collections. As described earlier, concerns around purity of hit compounds from these libraries were addressed through resynthesis (>95% purity by HPLC) and reconfirmation of activity for a selection of the compounds. Compounds **50–53**, **55**, **57–59**, **61–63**, **65**, **71**, **72**, **75**, **76**, and **84** were synthesized in high-throughput medicinal chemistry (HTMC) parallel synthesis conducted by Takeda Pharmaceutical Company Limited and therefore only MS data were collected as per standard operating practice for this technique

(see Supporting Information 1). The majority (over 85%) of these HTMC compounds were later confirmed as >95% purity by HPLC. For all other synthesized compounds, including those advanced to *in vivo* evaluation, purity was >95% by HPLC.

Method A: Preparation of Compound 25. To a solution of 2-aminobenzamide (**23**) (10 g, 73.52 mmol) and pyridine-2-carboxylic acid (**24**) (13.56 g, 110.3 mmol) in DMF (100 mL) were added HOBT (14.9 g, 110.3 mmol), EDCI (21.14 g, 110.3 mmol), and TEA (10.14 mL, 80.88 mmol). The reaction mixture was stirred for 24 h at room temperature. After TLC showed completion of the reaction, the reaction mixture was concentrated, water was added, and the formed precipitate was filtered, washed with water, and dried to afford *N*-(2-carbamoylphenyl)pyridine-2-carboxamide (**25**) (15 g, 84.6%) as a white solid. MS (ESI): *m/z* 242 [M + H]⁺.

Method B: Preparation of Compound 26. To a solution of **25** (18 g, 74.68 mmol) in methanol, 240 mL of 1 N NaOH (aqueous) was added and refluxed for 1 h. After TLC showed completion of the reaction, the reaction mixture was concentrated and diluted with water and neutralized with conc HCl to give a precipitate that was filtered, washed with water, and dried to afford 2-(pyridin-2-yl)quinazolin-4-ol (**26**) (11 g, 66.0%) as a white solid. MS (ESI): *m/z* 224 [M + H]⁺.

Method C: Preparation of Compound 27. To a solution of **26** (2 g, 8.97 mmol) in toluene (20 mL), TEA (7.5 mL) and POCl₃ (13 mL) were added and refluxed at 130 °C overnight. After completion of the reaction (monitored by TLC), toluene and POCl₃ were distilled and the residue obtained was diluted with DCM and washed with cold water and cold saturated NaHCO₃ solution. The organic layer was dried over Na₂SO₄, concentrated in vacuo, and purified by column chromatography (using silica gel 100–200 mesh, 15–20% EtOAc/hexane as the eluent) to afford 4-chloro-2-(pyridin-2-yl)quinazoline (**27**) (1.8 g, 83.1%) as a white solid. ¹H NMR (400 MHz, DMSO-*d*₆) δ 8.82–8.81 (d, 1H), 8.53–8.51 (d, 1H), 8.35–8.33 (d, 1H), 8.23–8.15 (m, 2H), 8.06–8.02 (t, 1H), 7.94–7.90 (t, 1H), 7.61–7.58 (m, 1H). MS (ESI): *m/z* 242 [M + H]⁺.

Method D: Preparation of Final Compounds (45–59, 61–63, 65–85, 85-tR1, 85-tR2, 87, 89, 90). Procedure A: **27** (250 mg, 1.04 mmol) and 3-phenylpyrrolidine (153 mg, 1.04 mmol) were mixed together in *n*-butanol (8 mL), and the reaction mixture was stirred at 110 °C for 12 h. After TLC showed completion of the reaction, the reaction mixture was concentrated and the residue was purified by prep HPLC to afford 4-(3-phenylpyrrolidin-1-yl)-2-(pyridin-2-yl)quinazoline (**80**) (86 mg, 23.5%) as a white solid. ¹H NMR (400 MHz, DMSO-*d*₆) δ 8.72–8.71 (d, 1H), 8.46–8.44 (d, 1H), 8.37–8.35 (d, 1H), 7.94–7.90 (dt, 1H), 7.86–7.78 (m, 2H), 7.50–7.35 (m, 6H), 7.29–7.26 (t, 1H), 4.42–4.37 (m, 1H), 4.18–4.16 (d, 2H), 4.01–3.96 (t, 1H), 3.59–3.55 (m, 1H), 2.43–2.40 (m, 1H), 2.23–2.18 (m, 1H). MS (ESI): *m/z* 353 [M + H]⁺. Procedure B: A mixture of **27** (450 mg, 1.86 mmol), 2-(pyrrolidin-3-yl)pyridine (**30**) (331 mg, 2.23 mmol), and DIEA (0.975 mL, 5.58 mmol) in MeCN (12 mL) was stirred at 120 °C for 30 min under microwave irradiation. The mixture was concentrated in vacuo, and the residue was purified by column chromatography (NH silica gel, 0–20% MeOH in EtOAc as the eluent), then crystallized from EtOAc-hexane to give 2-(pyridin-2-yl)-4-(3-(pyridin-2-yl)pyrrolidin-1-yl)quinazoline (**85**) (560 mg, 85%) as a white solid. ¹H NMR (300 MHz, DMSO-*d*₆) δ 8.74–8.69 (m, 1H), 8.60–8.54 (m, 1H), 8.48–8.42 (m, 1H), 8.37 (d, 1H), 7.96–7.90 (m, 1H), 7.88–7.75 (m, 3H), 7.54–7.43 (m, 3H), 7.33–7.25 (m, 1H), 4.46–4.36 (m, 1H), 4.29–4.12 (m, 3H), 3.83–3.69 (m, 1H), 2.47–2.40 (m, 1H), 2.38–2.24 (m, 1H). ¹³C NMR (75 MHz, DMSO-*d*₆) δ 160.8, 159.9, 158.8, 156.5, 152.5, 149.7, 137.3, 137.2, 137.1, 132.8, 128.6, 126.3, 125.5, 124.8, 124.0, 123.0, 122.6, 115.4, 56.0, 51.0, 45.4, 31.9. Anal. calcd for C₂₂H₁₉N₅: C 74.8, H 5.4, N 19.8. Found: C 75.3, H 4.9, N 20.3. HRMS (ESI): *m/z* 354.171 [M + H]⁺ (exact mass 353.164).

Method E: Preparation of Compound 29a. To a solution of 2,4-dichloro-5H-pyrrolo[3,2-*d*]pyrimidine (**28**) (1.20 g, 6.38 mmol) and ethyl iodide (2.95 g, 18.91 mmol) in DMF (20 mL), Cs₂CO₃ (5.20 g, 15.96 mmol) was added at room temperature. The mixture was stirred at room temperature under N₂ overnight. After concentration in vacuo, the residue was extracted with EtOAc. The organic layer was separated,

washed with water and brine, dried over MgSO_4 , and concentrated in vacuo. The residue was purified by column chromatography (silica gel, 30–50% EtOAc in hexane as the eluent) to give 2,4-dichloro-5-ethyl-5H-pyrrolo[3,2-d]pyrimidine (**29a**) (0.956 g, 69.3%) as a white solid. $^1\text{H NMR}$ (300 MHz, CDCl_3) δ 7.54 (d, 1H), 6.66 (d, 1H), 4.52 (q, 2H), 1.54 (t, 3H). MS (ESI): m/z 216, 218 $[\text{M} + \text{H}]^+$.

2,4-Dichloro-5-methyl-5H-pyrrolo[3,2-d]pyrimidine (29b). The title compound (602 mg, 70.0%) was synthesized from **28** according to method E as a white solid. $^1\text{H NMR}$ (300 MHz, CDCl_3) δ 7.45 (d, 1H), 6.64 (d, 1H), 4.14 (s, 3H). MS (ESI): m/z 202, 204 $[\text{M} + \text{H}]^+$.

Method F: Preparation of Compound 31a. To a solution of 2-(pyrrolidin-3-yl)pyridine (**30**) (297 mg, 2.00 mmol) and DIEA (0.875 mL, 5.01 mmol) in THF (8 mL) was added a solution of **29a** (360 mg, 1.67 mmol) in THF (4 mL) at room temperature. The mixture was stirred at room temperature for 10 h. After concentration in vacuo, the residue was purified by column chromatography (NH silica gel, 30–100% EtOAc/hexane as the eluent) to give 2-chloro-5-ethyl-4-(3-(pyridin-2-yl)pyrrolidin-1-yl)-5H-pyrrolo[3,2-d]pyrimidine (**31a**) (421 mg, 77%) as a colorless oil. $^1\text{H NMR}$ (300 MHz, CDCl_3) δ 8.60–8.55 (m, 1H), 7.67–7.61 (m, 1H), 7.28–7.25 (m, 1H), 7.22 (d, 1H), 7.20–7.14 (m, 1H), 6.51 (d, 1H), 4.36–4.17 (m, 2H), 4.15–3.96 (m, 3H), 3.88–3.76 (m, 1H), 3.63–3.49 (m, 1H), 2.48–2.24 (m, 2H), 1.37 (t, 3H). MS (ESI): m/z 328 $[\text{M} + \text{H}]^+$.

2-Chloro-5-methyl-4-(3-(pyridin-2-yl)pyrrolidin-1-yl)-5H-pyrrolo[3,2-d]pyrimidine (31b). The title compound (330 mg, 70.8%) was synthesized from **29b** according to method F as a white solid. $^1\text{H NMR}$ (300 MHz, CDCl_3) δ 8.60–8.54 (m, 1H), 7.67–7.62 (m, 1H), 7.23 (d, 1H), 7.21–7.15 (m, 1H), 7.14 (d, 1H), 6.48 (d, 1H), 4.19–4.01 (m, 3H), 3.95 (s, 3H), 3.88–3.84 (m, 1H), 3.65–3.48 (m, 1H), 2.50–2.24 (m, 2H). MS (ESI): m/z 314 $[\text{M} + \text{H}]^+$.

6-Chloro-4-(3-(pyridin-2-yl)pyrrolidin-1-yl)-1H-pyrazolo[3,4-d]pyrimidine (39). The title compound (1.20 g, 80%) was synthesized from 4,6-dichloro-1H-pyrazolo[3,4-d]pyrimidine (**38**) according to method F as a crude product. $^1\text{H NMR}$ (400 MHz, $\text{DMSO}-d_6$) δ 13.50 (s, 1H), 8.55–8.52 (t, 1H), 8.19–8.17 (d, 1H), 7.80–7.77 (m, 1H), 7.47–7.41 (m, 1H), 7.30–7.25 (m, 1H), 4.25–3.66 (m, 5H), 2.49–2.33 (m, 2H). MS (ESI): m/z 301 $[\text{M} + \text{H}]^+$.

2-Chloro-6-(3-(pyridin-2-yl)pyrrolidin-1-yl)purine (43). The title compound (170 mg, 27%) was synthesized from 2,6-dichloro-9H-purine (**42**) according to method F as a crude product. $^1\text{H NMR}$ (400 MHz, $\text{DMSO}-d_6$) δ 13.08 (s, 1H), 8.53–8.52 (d, 1H), 8.10–8.07 (d, 1H), 7.78–7.74 (t, 1H), 7.42–7.40 (d, 1H), 7.28–7.25 (t, 1H), 4.67–3.67 (m, 5H), 2.32–2.17 (m, 2H). MS (ESI): m/z 301 $[\text{M} + \text{H}]^+$.

Method G: Preparation of Final Compounds (86, 88). A mixture of **31a** (84 mg, 0.26 mmol), (2-pyridine)cyclic-triethylborate lithium salt (109 mg, 0.51 mmol), $\text{Pd}_2(\text{dba})_3$ (24 mg, 0.03 mmol), cuprous chloride (13 mg, 0.13 mmol), butyl di-1-adamantylphosphine (19 mg, 0.05 mmol), and potassium *tert*-butoxide (86 mg, 0.77 mmol) in DME (2 mL) was heated at 120 °C for 3 h under microwave irradiation. The insoluble material was removed by filtration, and the filtrate was concentrated in vacuo. The residue was purified by column chromatography (NH silica gel, 0–10% MeOH in EtOAc as the eluent), then by preparative HPLC (L-Column 2 ODS, eluted with H_2O in acetonitrile containing 10 mM NH_4HCO_3). The desired fraction was concentrated in vacuo. The residue was dissolved in EtOAc, and the solution was dried over Na_2SO_4 and concentrated in vacuo to give 5-ethyl-2-(pyridin-2-yl)-4-(3-(pyridin-2-yl)pyrrolidin-1-yl)-5H-pyrrolo[3,2-d]pyrimidine (**88**) (18 mg, 19.0%) as a colorless amorphous solid. $^1\text{H NMR}$ (300 MHz, CDCl_3) δ 8.83–8.77 (m, 1H), 8.59 (d, 1H), 8.49 (d, 1H), 7.78–7.76 (m, 1H), 7.68–7.52 (m, 1H), 7.32–7.08 (m, 4H), 6.79–6.65 (m, 1H), 4.43–3.54 (m, 7H), 3.10–2.28 (m, 2H), 1.47–1.36 (m, 3H). MS (ESI): m/z 371 $[\text{M} + \text{H}]^+$.

5-Methyl-2-(pyridin-2-yl)-4-(3-(pyridin-2-yl)pyrrolidin-1-yl)-5H-pyrrolo[3,2-d]pyrimidine (86). The title compound (39 mg, 42.9%) was synthesized from **31b** according to method G as a colorless amorphous solid. $^1\text{H NMR}$ (300 MHz, $\text{DMSO}-d_6$) δ 8.66 (d, 1H), 8.54 (d, 1H), 8.33 (d, 1H), 7.91–7.81 (m, 1H), 7.80–7.71 (m, 1H), 7.59 (d, 1H), 7.46–7.34 (m, 2H), 7.26 (dd, 1H), 6.54 (d, 1H), 4.19–3.98 (m, 6H), 3.93–3.80 (m, 1H), 3.72–3.56 (m, 1H), 2.44–2.31 (m, 1H), 2.30–2.15 (m, 1H). MS (ESI): m/z 357 $[\text{M} + \text{H}]^+$.

Method H: Preparation of Compound 33. To a stirred solution of ethyl iodide (2.08 g, 13.37 mmol) and K_2CO_3 (2.19 g, 15.92 mmol) in DMF (30 mL) was added 4-nitro-1H-pyrazole-3-carboxylic acid (**32**) (1.0 g, 6.36 mmol). The reaction mixture was stirred at room temperature for 3 h. After completion of the reaction (monitored by TLC), it was filtered and the filtrate obtained was extracted with EtOAc and the combined organic layer was washed with water (50 mL). The organic layer was dried over Na_2SO_4 and concentrated in vacuo. The residue was purified by flash chromatography (using silica gel 100–200 mesh, 15–20% EtOAc/hexane as the eluent) to afford compound **33**, a mixture of regioisomers (ethyl 1-ethyl-4-nitropyrzole-3-carboxylate and ethyl 2-ethyl-4-nitropyrzole-3-carboxylate) (0.95 g, 70.0%) as a yellow oil. MS (ESI): m/z 214 $[\text{M} + \text{H}]^+$.

Method I: Preparation of Compounds 34 (a, b). To a solution of **33** (5 g, 23.34 mmol) in EtOH/ H_2O (4:1, 20 mL), iron powder (13.03 g, 233.64 mmol) and NH_4Cl (1.25 g, 23.36 mmol) were added and the mixture was refluxed for 2 h. After completion of the reaction (monitored by TLC), the insoluble material was removed by filtration through celite and the filtrate was concentrated in vacuo to obtain a solid residue. The residue was purified by flash chromatography (using silica gel 100–200 mesh, 15–20% EtOAc in hexane as the eluent) to afford ethyl 4-amino-2-ethylpyrazole-3-carboxylate (**34a**) (1.2 g, 28.0%) as a white solid and ethyl 4-amino-1-ethylpyrazole-3-carboxylate (**34b**) (1.8 g, 42.1%) as a white solid. The structure of **34b** was confirmed by NOE experiment. **34a:** $^1\text{H NMR}$ (400 MHz, $\text{DMSO}-d_6$) δ 7.02 (s, 1H), 4.95 (bs, 2H), 4.32–4.25 (m, 4H), 1.32–1.28 (t, 3H), 1.24–1.22 (t, 3H). MS (ESI): m/z 184 $[\text{M} + \text{H}]^+$. **34b:** $^1\text{H NMR}$ (400 MHz, $\text{DMSO}-d_6$) δ 7.16 (s, 1H), 4.65 (bs, 2H), 4.25–4.19 (q, 2H), 4.05–4.00 (q, 2H), 1.33–1.23 (m, 6H). MS (ESI): m/z 184 $[\text{M} + \text{H}]^+$.

Method J: Preparation of Compound 36a. To a solution of **34a** (1.2 g, 6.55 mmol) and picolinimidamide (**35**) (1.13 g, 7.2 mmol) in EtOH (30 mL) was added DIEA (4.2 mL, 26.20 mmol) and the mixture was refluxed at 150 °C for 12 h. After completion of the reaction (monitored by TLC), the reaction mixture was cooled and precipitates were filtered off, washed with hexane and water, and dried to give 1-ethyl-5-(pyridin-2-yl)pyrazolo[4,3-d]pyrimidin-7-ol (**36a**) (1.2 g, 75.9%) as a white solid. $^1\text{H NMR}$ (400 MHz, $\text{DMSO}-d_6$) δ 11.30 (bs, 1H), 8.73–8.72 (d, 1H), 8.52 (s, 1H), 8.35–8.34 (d, 1H), 8.05–8.02 (t, 1H), 7.61 (t, 1H), 4.42–4.37 (q, 2H), 1.51–1.47 (t, 3H). MS (ESI): m/z 242 $[\text{M} + \text{H}]^+$.

2-Ethyl-5-(pyridin-2-yl)pyrazolo[4,3-d]pyrimidin-7-ol (36b). The title compound (2.2 g, 92.8%) was synthesized from **34b** according to method J as a white solid. $^1\text{H NMR}$ (400 MHz, $\text{DMSO}-d_6$) δ 11.74 (bs, 1H), 8.72–8.71 (d, 1H), 8.34–8.32 (d, 1H), 8.10 (s, 1H), 8.04–8.01 (t, 1H), 7.62–7.59 (t, 1H), 4.62–4.57 (q, 2H), 1.44–1.40 (t, 3H). MS (ESI): m/z 242 $[\text{M} + \text{H}]^+$.

1-Methyl-5-(pyridin-2-yl)pyrazolo[4,3-d]pyrimidin-7-ol (36c). The title compound (438 mg, 49.8%) was synthesized from ethyl 4-amino-2-methylpyrazole-3-carboxylate (**34c**) according to method J as an off-white solid. $^1\text{H NMR}$ (300 MHz, $\text{DMSO}-d_6$) δ 11.78 (bs, 1H), 8.76–8.69 (m, 1H), 8.39–8.31 (m, 1H), 8.12 (s, 1H), 8.08–8.00 (m, 1H), 7.67–7.57 (m, 1H), 4.24 (s, 3H). MS (ESI): m/z 228 $[\text{M} + \text{H}]^+$.

Method K: Preparation of Compound 37a. To a stirred solution of **36a** (1.0 g, 4.149 mmol) in toluene (10 mL) was added POCl_3 (15 mL) in ice-cold condition. The resulting solution was heated to reflux for 2 h under N_2 . The reaction was monitored by TLC and LCMS. After completion, the reaction mixture was concentrated in vacuo. The crude residue was diluted with DCM and quenched with saturated cold NaHCO_3 solution (10 mL). The organic layer was separated and the aqueous layer was extracted with DCM (2 × 20 mL), and the combined organic layer was washed with water (30 mL) followed by brine (30 mL). The organic layer was dried over Na_2SO_4 and concentrated in vacuo. The residue was purified by flash chromatography (using silica gel 100–200 mesh, 15–20% EtOAc/hexane as the eluent) to afford 7-chloro-1-ethyl-5-(pyridin-2-yl)pyrazolo[4,3-d]pyrimidine (**37a**) (700 mg, 65%) as an off-white solid. $^1\text{H NMR}$ (400 MHz, $\text{DMSO}-d_6$) δ 8.76–8.75 (d, 1H), 8.63 (s, 1H), 8.41–8.39 (d, 1H), 8.02–7.98 (t, 1H), 7.55–7.53 (t, 1H), 4.79–4.74 (q, 2H), 1.51–1.40 (t, 3H).

7-Chloro-2-ethyl-5-(pyridin-2-yl)pyrazolo[4,3-*d*]pyrimidine (37b). The title compound (250 mg, 58%) was synthesized from **36b** according to method K as a sticky solid. $^1\text{H NMR}$ (400 MHz, $\text{DMSO-}d_6$) δ 9.16 (bs, 1H), 8.83 (m, 1H), 8.59 (m, 1H), 8.29 (m, 1H), 7.78 (m, 1H), 4.69–4.63 (q, 2H), 1.61–1.58 (t, 3H).

7-Chloro-1-methyl-5-(pyridin-2-yl)pyrazolo[4,3-*d*]pyrimidine (37c). The title compound (1.21 g, 87%) was synthesized from **36c** according to method K as an off-white solid. $^1\text{H NMR}$ (300 MHz, $\text{DMSO-}d_6$) δ 8.79–8.74 (m, 1H), 8.60 (s, 1H), 8.43–8.37 (m, 1H), 8.04–7.95 (m, 1H), 7.58–7.51 (m, 1H), 4.38 (s, 3H). MS (ESI): m/z 246 $[\text{M} + \text{H}]^+$.

Method L: Preparation of Compounds 40 (a, b). To a stirred solution of **39** (1.2 g, 4.0 mmol) in DMF (10 mL), NaH (0.32 g, 60%, 13 mmol) and ethyl iodide (0.482 mL) were added at 0 °C. The resulting mixture was stirred at 25 °C for 16 h. After completion (monitored by TLC), the reaction mixture was quenched with ice-cold water and extracted with EtOAc, and the combined organic layers were dried over Na_2SO_4 and concentrated in vacuo. The residue was purified by column chromatography (using silica gel 100–200 mesh, 10–15% EtOAc/hexane as the eluent) to get 6-chloro-1-ethyl-4-(3-(pyridin-2-yl)pyrrolidin-1-yl)-1H-pyrazolo[3,4-*d*]pyrimidine (**40a**) (635 mg, 48%) as a brown solid and 6-chloro-2-ethyl-4-(3-(pyridin-2-yl)pyrrolidin-1-yl)-1H-pyrazolo[3,4-*d*]pyrimidine (**40b**) (150 mg, 11%) as a brown solid. Structures of **40a** and **40b** were assigned based on the NOE experiment on final compound **91**. **40a:** $^1\text{H NMR}$ (400 MHz, $\text{DMSO-}d_6$) δ 8.55–8.52 (t, 1H), 8.20–8.19 (d, 1H), 7.80–7.76 (dd, 1H), 7.48–7.41 (m, 1H), 7.30–7.26 (m, 1H), 4.29–3.73 (m, 7H), 2.38–2.18 (m, 2H), 1.37–1.35 (t, 3H). MS (ESI): m/z 329 $[\text{M} + \text{H}]^+$. **40b:** $^1\text{H NMR}$ (400 MHz, $\text{DMSO-}d_6$) δ 8.67 (s, 1H), 8.55–8.52 (m, 1H), 7.80–7.76 (q, 1H), 7.47–7.41 (dd, 1H), 7.31–7.26 (m, 1H), 4.36–3.66 (m, 7H), 2.38–2.17 (m, 2H), 1.49–1.41 (t, 3H). MS (ESI): m/z 329 $[\text{M} + \text{H}]^+$.

2-Chloro-9-ethyl-6-(3-(pyridin-2-yl)pyrrolidin-1-yl)purine (44). The title compound (70 mg, 37%) was synthesized from **43** according to method L as a crude product. MS (ESI): m/z 329 $[\text{M} + \text{H}]^+$.

Method M: Preparation of Final Compounds (91–93). To a stirred solution of **40a** (635 mg, 1.94 mmol) in 1,4-dioxane (10 mL) was added Pd(PPh_3)₄ (225 mg, 0.194 mmol) followed by 2-(tributylstannyl)pyridine (**41**) (1.549 mL, 4.84 mmol) at room temperature. The reaction mixture was stirred at 120 °C for 16 h. After completion (monitored by TLC), the reaction mixture was quenched with ice-cold water and extracted with EtOAc. The combined organic layers were dried over MgSO_4 and concentrated in vacuo. The resultant crude material was purified by prep HPLC to afford 1-ethyl-6-(pyridin-2-yl)-4-(3-(pyridin-2-yl)pyrrolidin-1-yl)-1H-pyrazolo[3,4-*d*]pyrimidine (**93**) (200 mg, 27.8%) as an off-white solid. $^1\text{H NMR}$ (400 MHz, $\text{DMSO-}d_6$) δ 8.72–8.70 (d, 1H), 8.55 (s, 1H), 8.44–8.41 (t, 1H), 8.23–8.21 (d, 1H), 7.92–7.88 (t, 1H), 7.78 (t, 1H), 7.49–7.44 (m, 2H), 7.28–7.27 (m, 1H), 4.43–3.73 (m, 7H), 2.49–2.20 (m, 2H), 1.43–1.40 (t, 3H). MS (ESI): m/z 373 $[\text{M} + \text{H}]^+$.

2-Ethyl-6-(pyridin-2-yl)-4-(3-(pyridin-2-yl)pyrrolidin-1-yl)-2H-pyrazolo[3,4-*d*]pyrimidine (91). The title compound (18 mg, 10.6%) was synthesized from **40b** according to method M as an off-white solid. The structure of **91** was confirmed by NOE experiment. $^1\text{H NMR}$ (400 MHz, $\text{DMSO-}d_6$) δ 8.66 (s, 2H), 8.58–8.55 (m, 1H), 8.36 (d, 1H), 7.90–7.78 (m, 2H), 7.50–7.42 (m, 2H), 7.32–7.29 (m, 1H), 4.42–3.80 (m, 7H), 2.49–2.35 (m, 2H), 1.54–1.46 (m, 3H). MS (ESI): m/z 372 $[\text{M} + \text{H}]^+$.

9-Ethyl-2-(pyridin-2-yl)-6-(3-(pyridin-2-yl)pyrrolidin-1-yl)-9H-purine (92). The title compound (45 mg, 30.6%) was synthesized from **44** according to method M as an off-white solid. $^1\text{H NMR}$ (400 MHz, $\text{DMSO-}d_6$) δ 8.70 (s, 1H), 8.55–8.54 (d, 1H), 8.40–8.39 (d, 1H), 8.23–8.22 (m, 1H), 7.91–7.89 (m, 1H), 7.80–7.75 (m, 1H), 7.45–7.43 (m, 2H), 7.29–7.26 (m, 1H), 4.68–3.74 (m, 7H), 2.54–2.24 (m, 2H), 1.46–1.43 (t, 3H). MS (ESI): m/z 372 $[\text{M} + \text{H}]^+$.

N-(5-Methylpyridin-2-yl)-2-(pyridin-2-yl)quinazolin-4-amine (45). The title compound (35 mg, 9%) was synthesized from **27** according to method D as a yellow solid. $^1\text{H NMR}$ (400 MHz, $\text{DMSO-}d_6$) δ 15.92 (bs, 0.5H), 10.42 (bs, 0.5H), 8.89–8.71 (m, 2H), 8.54–7.24 (m, 9H), 2.33 (s, 3H). MS (ESI): m/z 314 $[\text{M} + \text{H}]^+$.

N-(6-Methylpyridin-3-yl)-2-(pyridin-2-yl)quinazolin-4-amine (46). The title compound (50 mg, 20%) was synthesized from **27** according to method D as an off-white solid. $^1\text{H NMR}$ (400 MHz, $\text{DMSO-}d_6$) δ 9.98 (s, 1H), 9.14 (s, 1H), 8.76 (s, 1H), 8.62–8.60 (d, 1H), 8.42–8.37 (t, 2H), 7.99–7.94 (m, 3H), 7.72–7.68 (m, 1H), 7.52–7.49 (m, 1H), 7.34–7.32 (d, 1H), 2.49 (s, 3H). MS (ESI): m/z 314 $[\text{M} + \text{H}]^+$.

N-(2,5-Dimethylpyridin-3-yl)-2-(pyridin-2-yl)quinazolin-4-amine (47). The title compound (11 mg, 18.1%) was synthesized from **27** according to method D as a pale yellow solid. $^1\text{H NMR}$ (300 MHz, $\text{DMSO-}d_6$) δ 9.83 (s, 1H), 8.68 (d, 1H), 8.53 (d, 1H), 8.26 (d, 1H), 8.09 (d, 1H), 7.96–7.83 (m, 3H), 7.74 (d, 1H), 7.71–7.60 (m, 1H), 7.47–7.40 (m, 1H), 2.41 (s, 3H), 2.34 (s, 3H). MS (ESI): m/z 328 $[\text{M} + \text{H}]^+$.

2-(Pyridin-2-yl)-N-((pyridin-2-yl)methyl)quinazolin-4-amine (48). The title compound (150 mg, 38%) was synthesized from **27** according to method D as a white solid. $^1\text{H NMR}$ (400 MHz, $\text{DMSO-}d_6$) δ 9.04–9.01 (t, 1H), 8.70–8.69 (d, 1H), 8.54–8.53 (d, 1H), 8.39–8.36 (d, 1H), 8.29–8.27 (d, 1H), 7.90–7.83 (m, 3H), 7.74–7.69 (m, 1H), 7.60–7.55 (m, 1H), 7.47–7.43 (m, 2H), 7.26–7.23 (m, 1H), 5.01–4.99 (d, 2H). MS (ESI): m/z 314 $[\text{M} + \text{H}]^+$.

2-(Pyridin-2-yl)-N-((pyridin-3-yl)methyl)quinazolin-4-amine (49). The title compound (76 mg, 19.5%) was synthesized from **27** according to method D as a light brown solid. $^1\text{H NMR}$ (400 MHz, $\text{DMSO-}d_6$) δ 8.98–8.96 (t, 1H), 8.73–8.72 (m, 2H), 8.44–8.43 (d, 1H), 8.40–8.38 (d, 1H), 8.32–8.30 (d, 1H), 7.94–7.90 (m, 2H), 7.85–7.80 (m, 2H), 7.58–7.54 (m, 1H), 7.48–7.45 (dd, 1H), 7.35–7.32 (dd, 1H), 4.92–4.91 (d, 2H). MS (ESI): m/z 314 $[\text{M} + \text{H}]^+$.

N-((3-Methylpyridin-2-yl)methyl)-2-(pyridin-2-yl)quinazolin-4-amine (50). The title compound (20.7 mg, 79%) was synthesized from **27** by HTMC parallel synthesis according to method D as a white solid. MS (ESI): m/z 328 $[\text{M} + \text{H}]^+$.

N-((6-Methylpyridin-2-yl)methyl)-2-(pyridin-2-yl)quinazolin-4-amine (51). The title compound (19.9 mg, 74.8%) was synthesized from **27** by HTMC parallel synthesis according to method D as a white solid. MS (ESI): m/z 328 $[\text{M} + \text{H}]^+$.

2-(Pyridin-2-yl)-N-(2-(pyridin-2-yl)ethyl)quinazolin-4-amine (52). The title compound (15.8 mg, 53.7%) was synthesized from **27** by HTMC parallel synthesis according to method D as a white solid. MS (ESI): m/z 328 $[\text{M} + \text{H}]^+$.

2-(Pyridin-2-yl)-N-(1-(pyridin-2-yl)ethyl)quinazolin-4-amine (53). The title compound (20.9 mg, 79.8%) was synthesized from **27** by HTMC parallel synthesis according to method D as a white solid. MS (ESI): m/z 328 $[\text{M} + \text{H}]^+$.

2-(Pyridin-2-yl)-N-(2-(pyridin-2-yl)propan-2-yl)quinazolin-4-amine (54). The title compound (246 mg, 58%) was synthesized from **27** according to method D as a white solid. $^1\text{H NMR}$ (300 MHz, $\text{DMSO-}d_6$) δ 8.62 (d, 1H), 8.59–8.52 (m, 2H), 8.39 (s, 1H), 7.87–7.78 (m, 2H), 7.77–7.69 (m, 1H), 7.68–7.46 (m, 4H), 7.37 (dd, 1H), 7.16 (dd, 1H), 1.89 (s, 6H). $^{13}\text{C NMR}$ (75 MHz, $\text{DMSO-}d_6$) δ 165.5, 158.3, 158.0, 157.6, 155.4, 149.8, 148.8, 147.5, 136.1, 136.0, 132.4, 128.0, 125.4, 123.9, 122.9, 120.8, 119.1, 114.1, 58.0, 27.3, 27.9. Anal. calcd for $\text{C}_{21}\text{H}_{20}\text{N}_5$: C 73.9, H 5.6, N 20.5. Found: C 73.5, H 5.2, N 20.0. HRMS (ESI): m/z 342.171 $[\text{M} + \text{H}]^+$ (exact mass 341.164).

2-(Pyridin-2-yl)-N-(1-(pyridin-2-yl)cyclopropyl)quinazolin-4-amine (55). The title compound (17.7 mg, 65.2%) was synthesized from **27** by HTMC parallel synthesis according to method D as a white solid. MS (ESI): m/z 340 $[\text{M} + \text{H}]^+$.

N-[(1-Methylpyrazol-4-yl)methyl]-2-(pyridin-2-yl)quinazolin-4-amine (56). The title compound (21 mg, 5.3%) was synthesized from **27** according to method D as a light brown solid. $^1\text{H NMR}$ (400 MHz, $\text{DMSO-}d_6$) δ 8.76–8.75 (d, 1H), 8.71–8.69 (t, 1H), 8.49–8.47 (d, 1H), 8.28–8.26 (d, 1H), 7.97–7.93 (m, 1H), 7.83–7.77 (m, 3H), 7.53–7.47 (m, 3H), 4.69–4.67 (d, 2H), 3.75 (s, 3H). MS (ESI): m/z 317 $[\text{M} + \text{H}]^+$.

2-(Pyridin-2-yl)-N-(thiazol-2-ylmethyl)quinazolin-4-amine (57). The title compound (0.7 mg, 2.7%) was synthesized from **27** by HTMC parallel synthesis according to method D as a white solid. MS (ESI): m/z 320 $[\text{M} + \text{H}]^+$.

N-((1-Methyl-1H-imidazol-2-yl)methyl)-2-(pyridin-2-yl)quinazolin-4-amine (58). The title compound (13.8 mg, 54.5%) was

synthesized from **27** by HTMC parallel synthesis according to method D as a white solid. MS (ESI): m/z 317 [M + H]⁺.

N-(2-(1*H*-imidazol-1-yl)ethyl)-2-(pyridin-2-yl)quinazolin-4-amine (**59**). The title compound (21 mg, 83%) was synthesized from **27** by HTMC parallel synthesis according to method D as a white solid. MS (ESI): m/z 317 [M + H]⁺.

N-(Pyrazolo[1,5-*a*]pyridin-5-yl)-2-(pyridin-2-yl)quinazolin-4-amine (**61**). The title compound (5.1 mg, 18.8%) was synthesized from **27** by HTMC parallel synthesis according to method D as a white solid. MS (ESI): m/z 339 [M + H]⁺.

N-(Benzo[*d*]oxazol-2-ylmethyl)-2-(pyridin-2-yl)quinazolin-4-amine (**62**). The title compound (16.5 mg, 58.4%) was synthesized from **27** by HTMC parallel synthesis according to method D as a white solid. MS (ESI): m/z 354 [M + H]⁺.

N-(2-(1*H*-Benzo[*d*]imidazol-1-yl)ethyl)-2-(pyridin-2-yl)quinazolin-4-amine (**63**). The title compound (27.9 mg, 97.7%) was synthesized from **27** by HTMC parallel synthesis according to method D as a white solid. MS (ESI): m/z 367 [M + H]⁺.

1-(2-(Pyridin-2-yl)quinazolin-4-yl)piperidine-3-carbonitrile (**65**). The title compound (33 mg, 52.3%) was synthesized from **27** by HTMC parallel synthesis according to method D as a white solid. MS (ESI): m/z 316 [M + H]⁺.

1-(2-(Pyridin-2-yl)quinazolin-4-yl)piperidine-4-carbonitrile (**66**). The title compound (21 mg, 53.2%) was synthesized from **27** according to method D as a white solid. ¹H NMR (300 MHz, DMSO-*d*₆) δ 8.75 (d, 1H), 8.46 (dt, 1H), 8.05–7.83 (m, 4H), 7.61–7.47 (m, 2H), 4.08–3.97 (m, 2H), 3.69–3.57 (m, 2H), 3.25 (tt, 1H), 2.18–1.92 (m, 4H). MS (ESI): m/z 316 [M + H]⁺.

4-(3-Phenylpiperidin-1-yl)-2-(pyridin-2-yl)quinazoline (**67**). The title compound (65 mg, 89%) was synthesized from **27** according to method D as a white solid. ¹H NMR (300 MHz, DMSO-*d*₆) δ 8.81–8.68 (m, 1H), 8.44 (dt, 1H), 8.05 (d, 1H), 8.00–7.91 (m, 2H), 7.88–7.81 (m, 1H), 7.60–7.53 (m, 1H), 7.51–7.46 (m, 1H), 7.44–7.32 (m, 4H), 7.30–7.22 (m, 1H), 4.49 (t, 2H), 3.33–3.24 (m, 2H), 3.09 (bs, 1H), 2.13–1.80 (m, 4H). MS (ESI): m/z 367 [M + H]⁺.

2-(Pyridin-2-yl)-4-(3-(pyridin-2-yl)piperidin-1-yl)quinazoline (**68**). The title compound (27 mg, 59.2%) was synthesized from **27** according to method D as a white solid. ¹H NMR (300 MHz, DMSO-*d*₆) δ 8.73 (d, 1H), 8.55 (d, 1H), 8.45 (d, 1H), 8.06 (d, 1H), 7.98–7.91 (m, 2H), 7.87–7.74 (m, 2H), 7.59–7.53 (m, 1H), 7.51–7.41 (m, 2H), 7.29–7.25 (m, 1H), 4.61–4.49 (m, 2H), 3.47–3.39 (m, 1H), 3.28–3.16 (m, 2H), 2.13–2.07 (m, 1H), 1.99–1.90 (m, 3H). MS (ESI): m/z 368 [M + H]⁺.

4-Phenyl-1-[2-(pyridin-2-yl)quinazolin-4-yl]piperidin-4-ol (**69**). The title compound (50 mg, 19.2%) was synthesized from **27** according to method D as a white solid. ¹H NMR (400 MHz, DMSO-*d*₆) δ 8.77–8.76 (m, 1H), 8.49–8.47 (d, 1H), 8.14–8.12 (d, 1H), 7.96–7.94 (m, 2H), 7.87–7.84 (t, 1H), 7.57–7.51 (m, 4H), 7.36–7.32 (t, 2H), 7.25–7.23 (m, 1H), 5.26 (s, 1H), 4.43–4.41 (d, 2H), 3.72–3.66 (t, 2H), 2.32–2.22 (m, 2H), 1.83–1.80 (d, 2H). MS (ESI): m/z 383 [M + H]⁺.

4-(3,4-Dihydroisoquinolin-2(1*H*)-yl)-2-(pyridin-2-yl)quinazoline (**70**). The title compound (15.0 mg, 35.7%) was synthesized from **27** according to method D as a pale yellow amorphous powder. ¹H NMR (300 MHz, DMSO-*d*₆) δ 8.75 (d, 1H), 8.50 (dt, 1H), 8.17 (d, 1H), 8.00–7.83 (m, 3H), 7.62–7.47 (m, 2H), 7.32–7.18 (m, 4H), 5.04 (s, 2H), 4.11–4.07 (m, 2H), 3.16 (t, 2H). MS (ESI): m/z 339 [M + H]⁺.

4-(5,8-Dihydro-1,7-naphthyridin-7(6*H*)-yl)-2-(pyridin-2-yl)quinazoline (**71**). The title compound (24.4 mg, 81.2%) was synthesized from **27** by HTMC parallel synthesis according to method D as a white solid. MS (ESI): m/z 340 [M + H]⁺.

4-(7,8-Dihydro-1,6-naphthyridin-6(5*H*)-yl)-2-(pyridin-2-yl)quinazoline (**72**). The title compound (26.1 mg, 95.8%) was synthesized from **27** by HTMC parallel synthesis according to method D as a white solid. MS (ESI): m/z 340 [M + H]⁺.

4-(5,6-Dihydroimidazo[1,2-*a*]pyrazin-7(8*H*)-yl)-2-(pyridin-2-yl)quinazoline (**73**). The title compound (57 mg, 69.9%) was synthesized from **27** according to method D as a white solid. ¹H NMR (300 MHz, DMSO-*d*₆) δ 8.80–8.75 (m, 1H), 8.55–8.49 (m, 1H), 8.19 (d, 1H), 8.04–7.88 (m, 3H), 7.70–7.60 (m, 1H), 7.57–7.49 (m, 1H), 7.19 (d,

1H), 6.93 (d, 1H), 5.03 (s, 2H), 4.42–4.35 (m, 2H), 4.29–4.21 (m, 2H). MS (ESI): m/z 329 [M + H]⁺.

2-(Pyridin-2-yl)-4-(3,4,6,7-tetrahydro-5*H*-imidazo[4,5-*c*]pyridin-5-yl)quinazoline (**74**). The title compound (69 mg, 85%) was synthesized from **27** according to method D as a white solid. ¹H NMR (300 MHz, DMSO-*d*₆) δ 12.03–11.77 (m, 1H), 8.77 (dd, 1H), 8.50 (d, 1H), 8.20–8.08 (m, 1H), 8.04–7.82 (m, 3H), 7.66–7.56 (m, 1H), 7.56–7.46 (m, 2H), 4.93–4.77 (m, 2H), 4.12–4.08 (m, 2H), 3.11–2.90 (m, 2H). MS (ESI): m/z 329 [M + H]⁺.

2-(Pyridin-2-yl)-4-(4-(pyridin-2-yl)piperazin-1-yl)quinazoline (**75**). The title compound (23.5 mg, 79.7%) was synthesized from **27** by HTMC parallel synthesis according to method D as a white solid. MS (ESI): m/z 369 [M + H]⁺.

4-(4-(6-Methylpyridin-2-yl)piperazin-1-yl)-2-(pyridin-2-yl)quinazoline (**76**). The title compound (24.5 mg, 80.1%) was synthesized from **27** by HTMC parallel synthesis according to method D as a white solid. MS (ESI): m/z 383 [M + H]⁺.

1-(2-(Pyridin-2-yl)quinazolin-4-yl)pyrrolidine-3-carbonitrile (**77**). The title compound (34 mg, 56.4%) was synthesized from **27** according to method D as a pale yellow solid. ¹H NMR (300 MHz, DMSO-*d*₆) δ 8.79–8.67 (m, 1H), 8.47 (dt, 1H), 8.31 (d, 1H), 8.02–7.78 (m, 3H), 7.60–7.43 (m, 2H), 4.36–4.26 (m, 1H), 4.25–4.05 (m, 3H), 3.68–3.61 (m, 1H), 2.48–2.27 (m, 2H). MS (ESI): m/z 302 [M + H]⁺.

1-(2-(Pyridin-2-yl)quinazolin-4-yl)pyrrolidine-3-carboxamide (**78**). The title compound (35 mg, 73.3%) was synthesized from **27** according to method D as an off-white solid. ¹H NMR (300 MHz, DMSO-*d*₆) δ 8.73 (d, 1H), 8.45 (d, 1H), 8.33 (d, 1H), 7.99–7.90 (m, 1H), 7.88–7.75 (m, 2H), 7.59 (bs, 1H), 7.54–7.44 (m, 2H), 7.07 (bs, 1H), 4.23–3.97 (m, 4H), 3.17–3.06 (m, 1H), 2.33–2.05 (m, 2H). MS (ESI): m/z 320 [M + H]⁺.

1-(2-(Pyridin-2-yl)quinazolin-4-yl)pyrrolidine-3-carboxylic Acid (**79**). The title compound (33.0 mg, 26.5%) was synthesized from **27** according to method D as an off-white solid. ¹H NMR (300 MHz, DMSO-*d*₆) δ 8.74–8.69 (m, 1H), 8.44 (d, 1H), 8.31 (d, 1H), 7.97–7.89 (m, 1H), 7.86–7.73 (m, 2H), 7.52–7.43 (m, 2H), 4.22–3.89 (m, 4H), 3.07–2.93 (m, 1H), 2.26–2.07 (m, 2H). MS (ESI): m/z 321 [M + H]⁺.

4-(3-Phenoxypropyl)pyrrolidin-1-yl)-2-(pyridin-2-yl)quinazoline (**81**). The title compound (66 mg, 90%) was synthesized from **27** according to method D as a colorless amorphous powder. ¹H NMR (300 MHz, DMSO-*d*₆) δ 8.80–8.68 (m, 1H), 8.45 (dt, 1H), 8.36 (d, 1H), 8.02–7.73 (m, 3H), 7.58–7.43 (m, 2H), 7.37–7.25 (m, 2H), 7.10–6.91 (m, 3H), 5.25 (d, 1H), 4.38 (dd, 1H), 4.28–3.95 (m, 3H), 2.43–2.21 (m, 2H). MS (ESI): m/z 369 [M + H]⁺.

3-Phenyl-1-[2-(pyridin-2-yl)quinazolin-4-yl]pyrrolidin-3-ol (**82**). The title compound (80 mg, 50.6%) was synthesized from **27** according to method D as an off-white solid. ¹H NMR (400 MHz, DMSO-*d*₆) δ 8.72–8.71 (d, 1H), 8.46–8.44 (d, 1H), 8.37–8.35 (d, 1H), 7.95–7.91 (m, 1H), 7.87–7.78 (m, 2H), 7.66–7.64 (d, 2H), 7.51–7.45 (m, 2H), 7.43–7.39 (m, 2H), 7.33–7.29 (m, 1H), 5.58 (s, 1H), 4.36–4.14 (m, 4H), 2.50–2.45 (m, 1H), 2.27–2.23 (m, 1H). MS (ESI): m/z 369 [M + H]⁺.

4-[3-(4-Fluorophenyl)pyrrolidin-1-yl]-2-(pyridin-2-yl)quinazoline (**83**). The title compound (35 mg, 20.8%) was synthesized from **27** according to method D as an off-white solid. ¹H NMR (400 MHz, CDCl₃) δ 8.85–8.84 (d, 1H), 8.57–8.55 (d, 1H), 8.18–8.13 (m, 2H), 7.81–7.79 (t, 1H), 7.73–7.69 (t, 1H), 7.41–7.37 (t, 1H), 7.36–7.29 (m, 3H), 7.08–7.04 (t, 2H), 4.47–4.42 (m, 1H), 4.26–4.20 (m, 2H), 4.07–4.01 (t, 1H), 3.57–3.53 (m, 1H), 2.52–2.49 (m, 1H), 2.23–2.20 (m, 1H). MS (ESI): m/z 371 [M + H]⁺.

2-(Pyridin-2-yl)-4-(2-(pyridin-2-yl)pyrrolidin-1-yl)quinazoline (**84**). The title compound (14.6 mg, 51.6%) was synthesized from **27** by HTMC parallel synthesis according to method D as a white solid. MS (ESI): m/z 354 [M + H]⁺.

Chiral Isomer of 2-(Pyridin-2-yl)-4-(3-(pyridin-2-yl)pyrrolidin-1-yl)quinazoline 3-(Pyridin-2-yl)pyrrolidine-1-carboxylate (85-tR1). The title compound (118 mg, 90%) was synthesized from **27** and chiral amine **30-tR1** (see Supporting Information 1 for the preparation of chiral amines of **30**) according to method D as a white solid. ¹H NMR (300 MHz, DMSO-*d*₆) δ 8.75–8.70 (m, 1H), 8.59–8.54 (m, 1H), 8.48–8.42 (m, 1H), 8.36 (d, 1H), 7.97–7.89 (m, 1H), 7.88–7.76

(m, 3H), 7.54–7.43 (m, 3H), 7.32–7.28 (m, 1H), 4.46–4.33 (m, 1H), 4.29–4.13 (m, 3H), 3.83–3.68 (m, 1H), 2.48–2.39 (m, 1H), 2.39–2.24 (m, 1H). MS (ESI): m/z 354 [M + H]⁺.

Chiral Isomer of 2-(Pyridin-2-yl)-4-(3-(pyridin-2-yl)pyrrolidin-1-yl)quinazoline 3-(Pyridin-2-yl)pyrrolidine-1-carboxylate (85-tr2). The title compound (82 mg, 86%) was synthesized from 27 and chiral amine 30-tr2 (see Supporting Information 1 for the preparation of chiral amines of 30) according to method D as a white solid. ¹H NMR (300 MHz, DMSO-*d*₆) δ 8.75–8.70 (m, 1H), 8.59–8.54 (m, 1H), 8.48–8.42 (m, 1H), 8.37 (d, 1H), 7.97–7.90 (m, 1H), 7.88–7.76 (m, 3H), 7.54–7.43 (m, 3H), 7.32–7.28 (m, 1H), 4.45–4.35 (m, 1H), 4.28–4.13 (m, 3H), 3.83–3.69 (m, 1H), 2.48–2.40 (m, 1H), 2.39–2.24 (m, 1H). MS (ESI): m/z 354 [M + H]⁺.

1-Methyl-5-(pyridin-2-yl)-7-(3-(pyridin-2-yl)pyrrolidin-1-yl)-1H-pyrazolo[4,3-*d*]pyrimidine (87). The title compound (60 mg, 75%) was synthesized from 37c according to method D as a white solid. ¹H NMR (300 MHz, DMSO-*d*₆) δ 8.71–8.65 (m, 1H), 8.55 (d, 1H), 8.36 (d, 1H), 8.18 (s, 1H), 7.94–7.84 (m, 1H), 7.82–7.74 (m, 1H), 7.49–7.40 (m, 2H), 7.31–7.28 (m, 1H), 4.32–4.22 (m, 4H), 4.19–3.97 (m, 3H), 3.80–3.64 (m, 1H), 2.47–2.37 (m, 1H), 2.36–2.19 (m, 1H). MS (ESI): m/z 358 [M + H]⁺.

1-Ethyl-5-(pyridin-2-yl)-7-(3-(pyridin-2-yl)pyrrolidin-1-yl)-1H-pyrazolo[4,3-*d*]pyrimidine (89). The title compound (50 mg, 22.5%) was synthesized from 37a according to method D as an off-white solid. ¹H NMR (400 MHz, DMSO-*d*₆) δ 8.67 (bs, 1H), 8.54–8.53 (d, 1H), 8.35–8.33 (d, 1H), 8.23 (bs, 1H), 7.92–7.88 (t, 1H), 7.79–7.75 (t, 1H), 7.44–7.42 (d, 2H), 7.28–7.25 (m, 1H), 4.60–4.51 (m, 2H), 4.20–4.09 (m, 3H), 4.00–3.97 (m, 1H), 3.72–3.68 (m, 1H), 2.45–2.35 (m, 1H), 2.31–2.24 (m, 1H), 1.44–1.40 (t, 3H). MS (ESI): m/z 372 [M + H]⁺.

2-Ethyl-5-(pyridin-2-yl)-7-(3-(pyridin-2-yl)pyrrolidin-1-yl)-2H-pyrazolo[4,3-*d*]pyrimidine (90). The title compound (48 mg, 22.3%) was synthesized from 37b according to method D as an off-white solid. ¹H NMR (400 MHz, CDCl₃) δ 8.77 (bs, 1H), 8.60–8.59 (d, 1H), 8.54–8.50 (t, 1H), 8.01 (bs, 1H), 7.79–7.72 (m, 1H), 7.67–7.63 (m, 1H), 7.30–7.25 (m, 2H), 7.19–7.17 (m, 1H), 4.80–4.25 (m, 5H), 4.11–3.99 (m, 1H), 3.78–3.68 (m, 1H), 2.54–2.38 (m, 2H), 1.63–1.58 (t, 3H). MS (ESI): m/z 372 [M + H]⁺.

In Vitro Efficacy (Studies Conducted According to Conditions Reported Previously by This Team).³⁴ U2OS (human bone osteosarcoma host cells, ATCC, Manassas, VA) cells were cultured in DMEM-high glucose media (Welgene Inc., Gyeongsangbuk-do, Republic of Korea) supplemented with 10% (v/v) fetal bovine serum (FBS) (Gibco, Waltham, MA), 1% (v/v) penicillin–streptomycin (10,000 U/mL) (Gibco) at 37 °C, 5% CO₂. *T. cruzi* parasites used for the infection were Tissue Culture Trypomastigotes (TCT). To generate this stage of parasites, metacyclic trypomastigotes were obtained from a late-stage epimastigote culture. The metacyclic trypomastigotes were used to infect the monkey kidney cell line LLC-MK2 (ATCC). Parasites 7 days after infection were collected from the supernatant of the LLC-MK2 infected culture and reinfected new culture of LLC-MK2 in DMEM-low glucose media (Welgene Inc.) supplemented with 2% (v/v) FBS (Gibco), 1% (v/v) penicillin–streptomycin (10,000 U/mL) (Gibco). The compounds were prepared in 2-fold serial dilution 10 points from 10 mM (200× stock) with 100% DMSO (v/v) (Sigma-Aldrich, St. Louis, MO) into 384-well polypropylene microplates (Greiner Bio-One, Kremsmünster, Austria). For the controls, benznidazole (Carbosynth Ltd., Berkshire, U.K.) and posaconazole (Carbosynth Ltd.) were used as positive controls and 0.5% DMSO (v/v) as negative control. The 0.3 μ L of compounds or reference compounds were dispensed in 10 μ L of DPBS (Welgene) containing wells of 384-well tissue culture microplate (Greiner) with CyBi-Well multichannel pipettor (Analytik Jena AG, Jena, Germany). U2OS cells and parasites were mixed in DMEM-low glucose media (Welgene Inc.) supplemented with 2% (v/v) FBS (Gibco) and 1% (v/v) penicillin–streptomycin (10,000 U/mL) (Gibco) at the multiplicity of infection (MOI) values of 12.5:1 parasite to host cell. The prepared cells and parasite mixtures were dispensed into the assay plate at 50 μ L/well and incubated for 72 h at 37 °C, 5% CO₂. After incubation, the cells and parasites were stained using 5 μ M DRAQ5 (Biostatus Ltd.,

Leicestershire, U.K.) in 4% paraformaldehyde (CureBio, Seoul, Republic of Korea). Cell images were acquired with the Operetta automated confocal microscope (PerkinElmer, Inc., Waltham, MA) at 635 nm excitation filter, 20× lens magnification. Four images per well were captured covering 45% of the well and analyzed with Columbus software (PerkinElmer). The number of cells and intracellular parasites were counted by the DRAQ5 stained nuclei of both host cells and parasites. The large host cell nuclei were first detected and the cytoplasm of the host cells was then identified by a cytoplasm detection script. The intracellular parasites were defined as spots within the host cell cytoplasm using spot analysis and host cells containing more than three spots were considered to be infected. The infection ratio was determined by the number of infected cells divided by the total number of cells and normalized values based on the positive and negative controls to 0 and 100% infection. To estimate EC₅₀ and CC₅₀ values, data were fitted to sigmoid dose–response one-site-fit model 205 (4 Parameter Logistic Model) of XLfit (IDBS, Guildford, U.K.) in MicroSoft Excel.

In Vivo Efficacy Study. We used *in vivo* bioluminescence imaging to monitor the therapeutic efficacy of compound 85 against acute-stage *T. cruzi* infections. Animal work was performed under United Kingdom Home Office project licenses (PPLs 70/8207) and approved by the LSHTM Animal Welfare and Ethical Review Board. Procedures were conducted in accordance with the United Kingdom Animals (Scientific Procedures) Act 1986 (ASPA). BALB/c female mice (aged 7–8 weeks) were purchased from Charles River (U.K.). Animals were maintained under specific pathogen-free conditions in individually ventilated cages. They experienced a 12 h light/dark cycle, with access to food and water *ad libitum*. Mice were infected via i.p. injection with 1×10^3 bioluminescent *T. cruzi* strain (CL Brener) that constitutively expressed the red-shifted luciferase PpyRE9h derived from SCID mouse (bred in-house) blood.⁵⁷ At the peak of parasitemia (14 days after infection), BALB/c mice ($n = 3$) were treated by the oral route, twice daily at 50 mg/kg for 5 days and monitored by bioluminescence imaging.⁵⁸

Experimental conditions for *in silico* screening, additional parasitology, microsomal stability, solubility, PAMPA and mouse PK, and preliminary tolerability studies can be found in Supporting Information 1.

■ ASSOCIATED CONTENT

Data Availability Statement

Full data set for all compounds explored in this series are available online as sdf file at <https://ndi.org/research-development/portfolio/drug-discovery-booster/>.

Supporting Information

The Supporting Information is available free of charge at <https://pubs.acs.org/doi/10.1021/acs.jmedchem.2c00775>.

Full experimental details for all procedures, analytical traces (NMR, LCMS), full SAR tables for all compounds with SMILES strings and purity data for all compounds, and virtual screening protocols (PDF)

Data table with SMILES (CSV)

■ AUTHOR INFORMATION

Corresponding Author

Benjamin Perry – *Drugs for Neglected Diseases Initiative, Geneva 1202, Switzerland*; Present Address: Medicxi Ventures, 10 Cours de Rive, 1204 Geneva, Switzerland; orcid.org/0000-0001-6715-4213; Email: bengperry@yahoo.co.uk

Authors

Taisuke Tawarashi – *Takeda Pharmaceutical Company Limited, Fujisawa, Kanagawa 251-8555, Japan*
Atsuko Ochida – *Takeda Pharmaceutical Company Limited, Fujisawa, Kanagawa 251-8555, Japan*

Yuichiro Akao – Takeda Pharmaceutical Company Limited, Fujisawa, Kanagawa 251-8555, Japan

Sachiko Itono – Takeda Pharmaceutical Company Limited, Fujisawa, Kanagawa 251-8555, Japan; Present Address: Acelead Drug Discovery Partners, Inc., Kanagawa 251-0012, Japan

Masahiro Kamaura – Takeda Pharmaceutical Company Limited, Fujisawa, Kanagawa 251-8555, Japan; Present Address: Nissan Chemical Corporation, Chiba 274-0069, Japan.

Thamina Akther – Takeda Pharmaceutical Company Limited, Fujisawa, Kanagawa 251-8555, Japan; Present Address: University of Minnesota, Minneapolis, Minnesota 55455, United States.

Mitsuyuki Shimada – Takeda Pharmaceutical Company Limited, Fujisawa, Kanagawa 251-8555, Japan; Present Address: The University of Tokyo, 7-chōme-3-1 Hongō, Bunkyo City, Tokyo 113-8654, Japan.

Stacie Canan – Celgene Corporation, Celgene Global Health, San Diego, California 92121, United States; Present Address: Elgia Therapeutics, Inc., 7660 Fay Avenue, La Jolla, California 92037, United States.

Sanjoy Chowdhury – TCG Lifesciences, Kolkata 700091, India

Yafeng Cao – WuXi AppTec Company Ltd., Wuhan 430075, People's Republic of China

Kevin Condroski – Celgene Corporation, Celgene Global Health, San Diego, California 92121, United States; Present Address: Loxo Oncology at Lilly, 600 Tech Ct, Louisville, Colorado 80027, United States.; orcid.org/0000-0002-5801-9332

Ola Engkvist – AstraZeneca Discovery Sciences, R&D, 431 50 Mölndal, Sweden; orcid.org/0000-0003-4970-6461

Amanda Francisco – London School of Hygiene and Tropical Medicine, London WC1E 7HT, U.K.

Sunil Ghosh – TCG Lifesciences, Kolkata 700091, India

Rina Kaki – Shionogi & Co., Ltd, Toyonaka-shi, Osaka 561-0825, Japan

John M. Kelly – London School of Hygiene and Tropical Medicine, London WC1E 7HT, U.K.

Chiaki Kimura – Shionogi & Co., Ltd, Toyonaka-shi, Osaka 561-0825, Japan

Thierry Kogej – AstraZeneca Discovery Sciences, R&D, 431 50 Mölndal, Sweden

Kazuya Nagaoka – Eisai Co., Ltd, Tsukuba, Ibaraki 300-2635, Japan

Akira Naito – Shionogi & Co., Ltd, Toyonaka-shi, Osaka 561-0825, Japan

Garry Pairaudeau – AstraZeneca, Discovery Sciences, R&D, Cambridge CB4 0WG, U.K.; Present Address: Exscientia, Oxford Science Park, The Schrödinger Building, Oxford OX4 4GE, U.K.

Constantin Radu – Institut Pasteur Korea, Seongnam-si, Gyeonggi-do 13488, Republic of Korea; Present Address: Molecular Devices, 3860 N First Street, San Jose, California 95134, United States

Ieuan Roberts – AstraZeneca, Discovery Sciences, R&D, Cambridge CB4 0WG, U.K.

David Shum – Institut Pasteur Korea, Seongnam-si, Gyeonggi-do 13488, Republic of Korea

Nao-aki Watanabe – Eisai Co., Ltd, Tsukuba, Ibaraki 300-2635, Japan

Huanxu Xie – WuXi AppTec Company Ltd., Wuhan 430075, People's Republic of China

Shuji Yonezawa – Shionogi & Co., Ltd, Toyonaka-shi, Osaka 561-0825, Japan

Osamu Yoshida – Shionogi & Co., Ltd, Toyonaka-shi, Osaka 561-0825, Japan

Ryu Yoshida – Shionogi & Co., Ltd, Toyonaka-shi, Osaka 561-0825, Japan

Charles Mowbray – Drugs for Neglected Diseases Initiative, Geneva 1202, Switzerland; orcid.org/0000-0003-3538-8116

Complete contact information is available at:

<https://pubs.acs.org/10.1021/acs.jmedchem.2c00775>

Author Contributions

O.E., T.K., K.C., K.N., H.N., S.Y., and S.I. performed *in silico* virtual screening at the respective partners; B.P., T.Y., T.T., A.O., H.X., Y.C., and S.G. guided the chemical synthesis; D.S. and C.R. performed *in vitro* parasitology assays; A.F. and J.K. performed *in vivo* efficacy, B.P., T.A., T.T., and A.O. guided the medicinal chemistry design, B.P., C.R., I.R., S.C., C.K., O.Y., R.Y., Y.A., and N.W. coordinated the Booster project at the respective partners; C.M., B.P., G.P., N.W., A.N., and M.S. conceived and implemented the Booster project; and T.T., T.A., and B.P. prepared the manuscript.

Funding

This work and the NTD drug discovery booster were funded by Global Health Innovation Technology Fund (GHIT) grants H2014-201, H2016-203, and H2017-001. The work was benefitted from generous in-kind contributions of resource from Takeda Pharmaceutical Company Limited, Eisai Co. Ltd., Shionogi & Co. Ltd., AstraZeneca plc, and Celgene Corporation.

Notes

The authors declare no competing financial interest.

ACKNOWLEDGMENTS

The authors acknowledge John Cuff, Leelapavan Tadoori, Jean Robert Ioset, Tatsuro Kuzuki, Daisuke Imoto, Midori Morioka, Dominique Junod, and Jean Pierre Paccaud for their help in implementation and logistics of the Booster project, Chen Min and Jiajia Zhang for ADME-PK studies, Sudin Panja and Ujjwal Pahari for contributions to synthesis, Jen Riley for the TcCYP51 assay data, and Louise Burrows for help in the manuscript preparation. The authors also acknowledge the generous support of Global Health Innovative Technology Fund (GHIT) for financial support of this project, and our collaboration partners at Abbvie Inc., Astellas Pharma Inc., and Merck KGaA for participation in the Booster project outside of this particular series. The authors thank the Abbvie Inc. for the off-target liability screen. The Drugs for Neglected Diseases initiative (DNDi) is grateful to its donors, public and private, who have provided funding to DNDi since its inception in 2003. A full list of DNDi's donors can be found at <http://www.dndi.org/donors/donors/>.

ABBREVIATIONS

5HT-1A, serotonin receptor 1A; BID, bis in die; CD, Chagas Disease; HCS, high-content screening; HTMC, high-throughput medicinal chemistry (parallel synthesis); HTS, high-throughput screening; LCMS, liquid chromatography-mass spectrometry; NMR, nuclear magnetic resonance; NTD, neglected tropical disease; PAMPA, parallel artificial membrane

permeability assay; PoC, proof of concept; SAR, structure–activity relationship; SD, standard deviation

REFERENCES

- (1) Field, M. C.; Horn, D.; Fairlamb, A. H.; Ferguson, M. A. J.; Gray, D. W.; Read, K. D.; de Rycker, M.; Torrie, L. S.; Wyatt, P. G.; Wyllie, S.; Gilbert, I. H. Anti-Trypanosomatid Drug Discovery: An Ongoing Challenge and a Continuing Need. *Nat. Rev. Microbiol.* **2017**, *15*, 217–231.
- (2) WHO. *Investing to Overcome the Global Impact of Neglected Tropical Diseases*; WHO, 2016.
- (3) McCall, L. I.; McKerrow, J. H. Determinants of Disease Phenotype in Trypanosomatid Parasites. *Trends Parasitol.* **2014**, *30*, 342–349.
- (4) Irish, A.; Whitman, J. D.; Clark, E. H.; Marcus, R.; Bern, C. Updated Estimates and Mapping for Prevalence of Chagas Disease among Adults, United States. *Emerg Infect Dis.* **2022**, *28*, 1313–1320.
- (5) Ferreira, M. S.; Borges, A. S. Some Aspects of Protozoan Infections in Immunocompromised Patients - A Review. *Mem. Inst. Oswaldo Cruz* **2002**, *97*, 443–457.
- (6) da Mata, J. R.; da Mata, F. R.; do Nascimento, G. N. L.; Ferreira, T. A. A. Pequeno Comprometimento de Encéfalo Em Ratos Holtzman Imunossuprimidos e Infectados Por *Trypanosoma cruzi*. *Acta Sci. Health Sci.* **2009**, *31*, 45–50.
- (7) Gascon, J.; Bern, C.; Pinazo, M. J. Chagas Disease in Spain, the United States and Other Non-Endemic Countries. *Acta Trop.* **2010**, *115*, 22–27.
- (8) WHO. Chagas disease. https://www.who.int/chagas/home_more/en/ (accessed June 12, 2020).
- (9) Briceño-León, R.; Galván, J. M. The Social Determinants of Chagas Disease and the Transformations of Latin America. *Mem. Inst. Oswaldo Cruz* **2007**, *102*, 109–112.
- (10) Pérez-Molina, J. A.; Norman, F.; López-Vélez, R. Chagas Disease in Non-Endemic Countries: Epidemiology, Clinical Presentation and Treatment. *Curr. Infect. Dis. Rep.* **2012**, *14*, 263–274.
- (11) Abad-Franch, F.; Lima, M. M.; Sarquis, O.; Gurgel-Gonçalves, R.; Sánchez-Martín, M.; Calzada, J.; Saldaña, A.; Monteiro, F. A.; Palomeque, F. S.; Santos, W. S.; Angulo, V. M.; Esteban, L.; Dias, F. B. S.; Diotaiuti, L.; Bar, M. E.; Gottdenker, N. L. On Palms, Bugs, and Chagas Disease in the Americas. *Acta Trop.* **2015**, *151*, 126–141.
- (12) Aguilar, H. M.; Abad-Franch, F.; Dias, J. C. P.; Junqueira, A. C. V.; Coura, J. R. Chagas Disease in the Amazon Region. *Mem. Inst. Oswaldo Cruz* **2007**, *102*, 47–55.
- (13) Coura, J. R.; Vias, P. A. Chagas Disease: A New Worldwide Challenge. *Nature* **2010**, *465*, S6–S7.
- (14) de Rycker, M.; Baragaña, B.; Duce, S. L.; Gilbert, I. H. Challenges and Recent Progress in Drug Discovery for Tropical Diseases. *Nature* **2018**, *559*, 498–506.
- (15) Carabarin-Lima, A.; González-Vázquez, M. C.; Rodríguez-Morales, O.; Baylón-Pacheco, L.; Rosales-Encina, J. L.; Reyes-López, P. A.; Arce-Fonseca, M. Chagas Disease (American Trypanosomiasis) in Mexico: An Update. *Acta Trop.* **2013**, *127*, 126–135.
- (16) Scarim, C. B.; Jornada, D. H.; Chelucci, R. C.; de Almeida, L.; dos Santos, J. L.; Chung, M. C. Current Advances in Drug Discovery for Chagas Disease. *Eur. J. Med. Chem.* **2018**, *155*, 824–838.
- (17) Díaz, S.; Villavicencio, B.; Correia, N.; Costa, J.; Haag, K. L. Triatomine Bugs, Their Microbiota and *Trypanosoma cruzi*: Asymmetric Responses of Bacteria to an Infected Blood Meal. *Parasites Vectors* **2016**, *9*, 636.
- (18) Taylor, M. C.; Ward, A.; Olmo, F.; Jayawardhana, S.; Francisco, A. F.; Lewis, M. D.; Kelly, J. M. Intracellular DNA Replication and Differentiation of *Trypanosoma cruzi* Is Asynchronous within Individual Host Cells in Vivo at All Stages of Infection. *PLoS Neglected Trop. Dis.* **2020**, *14*, No. e0008007.
- (19) CDC. Chagas Disease - Biology. <https://www.cdc.gov/parasites/chagas/biology.html> (accessed Nov 20, 2020).
- (20) Prata, A. Clinical and Epidemiological Aspects of Chagas Disease. *Lancet Infect. Dis.* **2001**, *1*, 92–100.
- (21) Carvalho, A. B.; Goldenberg, R. C. D. S.; Campos de Carvalho, A. C. Cell Therapies for Chagas Disease. *Cytotherapy* **2017**, *19*, 1339–1349.
- (22) Pecoul, B.; Batista, C.; Stobbaerts, E.; Ribeiro, I.; Vilasanjuan, R.; Gascon, J.; Pinazo, M. J.; Moriana, S.; Gold, S.; Pereiro, A.; Navarro, M.; Torrico, F.; Bottazzi, M. E.; Hotez, P. J. The BENEFIT Trial: Where Do We Go from Here? *PLoS Neglected Trop. Dis.* **2016**, *10*, No. e0004343.
- (23) Bern, C. Chagas' Disease. *N. Engl. J. Med.* **2015**, *373*, 456–466.
- (24) Molina, I.; Gómez i Prat, J.; Salvador, F.; Treviño, B.; Sulleiro, E.; Serre, N.; Pou, D.; Roure, S.; Cabezos, J.; Valerio, L.; Blanco-Grau, A.; Sánchez-Montalvá, A.; Vidal, X.; Pahissa, A. Randomized Trial of Posaconazole and Benznidazole for Chronic Chagas' Disease. *N. Engl. J. Med.* **2014**, *370*, 1899–1908.
- (25) Chatelain, E. Chagas Disease Drug Discovery: Toward a New Era. *SLAS Discovery* **2015**, *20*, 22–35.
- (26) Urbina, J. A.; Docampo, R. Specific Chemotherapy of Chagas Disease: Controversies and Advances. *Trends Parasitol.* **2003**, *19*, 495–501.
- (27) Coura, J. R.; De Castro, S. L. A Critical Review on Chagas Disease Chemotherapy. *Mem. Inst. Oswaldo Cruz* **2002**, *97*, 3–24.
- (28) Sykes, M. L.; Avery, V. M. 3-Pyridyl Inhibitors with Novel Activity against *Trypanosoma cruzi* Reveal in Vitro Profiles Can Aid Prediction of Putative Cytochrome P450 Inhibition. *Sci. Rep.* **2018**, *8*, No. 4901.
- (29) Morillo, C. A.; Waskin, H.; et al. Benznidazole and Posaconazole in Eliminating Parasites in Asymptomatic *T. cruzi* Carriers: The STOP-CHAGAS Trial. *J. Am. Coll. Cardiol.* **2017**, *69*, 939–947.
- (30) Morillo, C. A.; Marin-Neto, J. A.; Avezum, A.; Sosa-Estani, S.; Rassi, A.; Rosas, F.; Villena, E.; Quiroz, R.; Bonilla, R.; Britto, C.; Guhl, F.; Velazquez, E.; Bonilla, L.; Meeks, B.; Rao-Melacini, P.; Pogue, J.; Mattos, A.; Lazdins, J.; Rassi, A.; Connolly, S. J.; Yusuf, S. Randomized Trial of Benznidazole for Chronic Chagas' Cardiomyopathy. *N. Engl. J. Med.* **2015**, *373*, 1295–1306.
- (31) Torrico, F.; Gascon, J.; Ortiz, L.; Alonso-Vega, C.; Pinazo, M.-J.; Schijman, A.; Almeida, I. C.; Alves, F.; et al. Treatment of Adult Chronic Indeterminate Chagas Disease with Benznidazole and Three E1224 Dosing Regimens: A Proof-of-Concept, Randomised, Placebo-Controlled Trial. *Lancet Infect. Dis.* **2018**, *18*, 419–430.
- (32) Franco, C. H.; Warhurst, D. C.; Bhattacharyya, T.; Au, H. Y. A.; Le, H.; Giardini, M. A.; Pascoalino, B. S.; Torrecilhas, A. C.; Romera, L. M. D.; Madeira, R. P.; Schenkman, S.; Freitas-Junior, L. H.; Chatelain, E.; Miles, M. A.; Moraes, C. B. Novel Structural CYP51 Mutation in *Trypanosoma cruzi* Associated with Multidrug Resistance to CYP51 Inhibitors and Reduced Infectivity. *Int. J. Parasitol.: Drugs Drug Resist.* **2020**, *13*, 107–120.
- (33) Nagle, A. S.; Khare, S.; Kumar, A. B.; Supek, F.; Buchynskyy, A.; Mathison, C. J. N.; Chennamaneni, N. K.; Pendem, N.; Buckner, F. S.; Gelb, M. H.; Molteni, V. Recent Developments in Drug Discovery for Leishmaniasis and Human African Trypanosomiasis. *Chem. Rev.* **2014**, *114*, 11305–11347.
- (34) Khare, S.; Nagle, A. S.; Biggart, A.; Lai, Y. H.; Liang, F.; Davis, L. C.; Barnes, S. W.; Mathison, C. J. N.; Myburgh, E.; Gao, M. Y.; Gillespie, J. R.; Liu, X.; Tan, J. L.; Stinson, M.; Rivera, I. C.; Ballard, J.; Yeh, V.; Groessl, T.; Federe, G.; Koh, H. X. Y.; Venable, J. D.; Bursulaya, B.; Shapiro, M.; Mishra, P. K.; Spraggon, G.; Brock, A.; Mottram, J. C.; Buckner, F. S.; Rao, S. P. S.; Wen, B. G.; Walker, J. R.; Tuntland, T.; Molteni, V.; Glynne, R. J.; Supek, F. Proteasome Inhibition for Treatment of Leishmaniasis, Chagas Disease and Sleeping Sickness. *Nature* **2016**, *537*, 229–233.
- (35) Varghese, S.; Rahmani, R.; Russell, S.; Deora, G. S.; Ferrins, L.; Toynton, A.; Jones, A.; Sykes, M.; Kessler, A.; Eufrásio, A.; Cordeiro, A. T.; Sherman, J.; Rodriguez, A.; Avery, V. M.; Piggott, M. J.; Baell, J. B. Discovery of Potent N-Ethylurea Pyrazole Derivatives as Dual Inhibitors of *Trypanosoma brucei* and *Trypanosoma cruzi*. *ACS Med. Chem. Lett.* **2020**, *11*, 278–285.
- (36) Villalta, F.; Rachakonda, G. Advances in Preclinical Approaches to Chagas Disease Drug Discovery. *Expert Opin. Drug Discovery* **2019**, *14*, 1161–1174.

- (37) Klug, D. M.; Diaz-Gonzalez, R.; DeLano, T. J.; Mavrogiannaki, E. M.; Buskes, M. J.; Dalton, R. M.; Fisher, J. K.; Schneider, K. M.; Hilborne, V.; Fritsche, M. G.; Simpson, Q. J.; Tear, W. F.; Devine, W. G.; Pérez-Moreno, G.; Ceballos-Pérez, G.; García-Hernández, R.; Bosch-Navarrete, C.; Ruiz-Pérez, L. M.; Gamarro, F.; González-Pacanowska, D.; Martínez-Martínez, M. S.; Manzano-Chinchon, P.; Navarro, M.; Pollastri, M. P.; Ferrins, L. Structure–Property Studies of an Imidazoquinoline Chemotype with Antitrypanosomal Activity. *RSC Med. Chem.* **2020**, *11*, 950–959.
- (38) Sear, C. E.; Pieper, P.; Amaral, M.; Romanelli, M. M.; Costa-Silva, T. A.; Haugland, M. M.; Tate, J. A.; Lago, J. H. G.; Tempone, A. G.; Anderson, E. A. Synthesis and Structure–Activity Relationship of Dehydrodieugenol B Neolignans against *Trypanosoma cruzi*. *ACS Infect. Dis.* **2020**, *6*, 2872–2878.
- (39) Lima, M. L.; Tulloch, L. B.; Corpas-Lopez, V.; Carvalho, S.; Wall, R. J.; Milne, R.; Rico, E.; Patterson, S.; Gilbert, I. H.; Moniz, S.; MacLean, L.; Torrie, L. S.; Morgillo, C.; Horn, D.; Zuccotto, F.; Wyllie, S. Identification of a Proteasome-Targeting Arylsulfonamide with Potential for the Treatment of Chagas' Disease. *Antimicrob. Agents Chemother.* **2022**, *66*, No. e01535-21.
- (40) de Rycker, M.; Wyllie, S.; Horn, D.; Read, K. D.; Gilbert, I. H. Anti-Trypanosomatid Drug Discovery: Progress and Challenges. *Nat. Rev. Microbiol.* **2023**, *21*, 35–50.
- (41) Screening Chagas disease | DNDi. <https://dndi.org/research-development/portfolio/screening-chagas/> (accessed March 31, 2021).
- (42) NTD Drug Discovery Booster Hit-to-lead | DNDi. <https://dndi.org/research-development/portfolio/drug-discovery-booster> (accessed Feb 03, 2021).
- (43) Akao, Y.; Canan, S.; Cao, Y.; Condroski, K.; Engkvist, O.; Itono, S.; Kaki, R.; Kimura, C.; Kogej, T.; Nagaoka, K.; Naito, A.; Nakai, H.; Pairaudeau, G.; Radu, C.; Roberts, I.; Shimada, M.; Shum, D.; Watanabe, N.; Xie, H.; Yonezawa, S.; Yoshida, O.; Yoshida, R.; Mowbray, C.; Perry, B. Collaborative Virtual Screening to Elaborate an Imidazo[1,2- a]Pyridine Hit Series for Visceral Leishmaniasis. *RSC Med. Chem.* **2021**, *12*, 384–393.
- (44) Hughes, J. P.; Rees, S. S.; Kalindjian, S. B.; Philpott, K. L. Principles of Early Drug Discovery. *Br. J. Pharmacol.* **2011**, *162*, 1239–1249.
- (45) Ripphausen, P.; Nisius, B.; Bajorath, J. State-of-the-Art in Ligand-Based Virtual Screening. *Drug Discovery Today* **2011**, *16*, 372–376.
- (46) Kogej, T.; Blomberg, N.; Greasley, P. J.; Mundt, S.; Vainio, M. J.; Schamberger, J.; Schmidt, G.; Hüser, J. Big Pharma Screening Collections: More of the Same or Unique Libraries? The AstraZeneca-Bayer Pharma AG Case. *Drug Discovery Today* **2013**, *18*, 1014–1024.
- (47) Orhan, I.; Şener, B.; Kaiser, M.; Brun, R.; Tasdemir, D. Inhibitory Activity of Marine Sponge-Derived Natural Products against Parasitic Protozoa. *Mar. Drugs* **2010**, *8*, 47–58.
- (48) SciFinder Discovery Platform | CAS. <https://www.cas.org/scifinder-discovery-platform> (accessed March 31, 2021).
- (49) Phan, T.-N.; Baek, K.-H.; Lee, N.; Byun, S. Y.; Shum, D.; No, J. H. In Vitro and in Vivo Activity of MTOR Kinase and PI3K Inhibitors Against *Leishmania donovani* and *Trypanosoma brucei*. *Molecules* **2020**, *25*, 1980.
- (50) Diaz-Gonzalez, R.; Kuhlmann, F. M.; Galan-Rodriguez, C.; da Silva, L. M.; Saldivia, M.; Karver, C. E.; Rodriguez, A.; Beverley, S. M.; Navarro, M.; Pollastri, M. P. The Susceptibility of Trypanosomatid Pathogens to PI3/MTOR Kinase Inhibitors Affords a New Opportunity for Drug Repurposing. *PLoS Neglected Trop. Dis.* **2011**, *5*, No. e1297.
- (51) Baell, J. B.; Holloway, G. A. New Substructure Filters for Removal of Pan Assay Interference Compounds (PAINS) from Screening Libraries and for Their Exclusion in Bioassays. *J. Med. Chem.* **2010**, *53*, 2719–2740.
- (52) Daina, A.; Michielin, O.; Zoete, V. SwissADME: A Free Web Tool to Evaluate Pharmacokinetics, Drug-Likeness and Medicinal Chemistry Friendliness of Small Molecules. *Sci. Rep.* **2017**, *7*, No. 42717.
- (53) Connolly, D. J.; Guiry, P. J. A Facile and Versatile Route to 2-Substituted-4(3H)-Quinazolinones and Quinazolines. *Synlett* **2001**, 1707–1710.
- (54) Riley, J.; Brand, S.; Voice, M.; Caballero, I.; Calvo, D.; Read, K. D. Development of a Fluorescence-Based *Trypanosoma cruzi* CYP51 Inhibition Assay for Effective Compound Triaging in Drug Discovery Programmes for Chagas Disease. *PLoS Neglected Trop. Dis.* **2015**, *9*, No. e0004014.
- (55) Meller, E.; Chalfin, M.; Bohmaker, K. Serotonin 5-HT_{1a} Receptor-Mediated Hypothermia in Mice: Absence of Spare Receptors and Rapid Induction of Tolerance. *Pharmacol., Biochem. Behav.* **1992**, *43*, 405–411.
- (56) Watanabe, A.; Mayumi, K.; Nishimura, K.; Osaki, H. In Vivo Use of the CYP Inhibitor 1-Aminobenzotriazole to Increase Long-Term Exposure in Mice. *Biopharm. Drug Dispos.* **2016**, *37*, 373–378.
- (57) Lewis, M. D.; Fortes Francisco, A.; Taylor, M. C.; Burrell-Saward, H.; Mclatchie, A. P.; Miles, M. A.; Kelly, J. M. Bioluminescence Imaging of Chronic *Trypanosoma cruzi* Infections Reveals Tissue-Specific Parasite Dynamics and Heart Disease in the Absence of Locally Persistent Infection. *Cell. Microbiol.* **2014**, *16*, 1285–1300.
- (58) Costa, F. C.; Francisco, A. F.; Jayawardhana, S.; Calderano, S. G.; Lewis, M. D.; Olmo, F.; Beneke, T.; Gluenz, E.; Sunter, J.; Dean, S.; Kelly, J. M.; Taylor, M. C. Expanding the Toolbox for *Trypanosoma cruzi*: A Parasite Line Incorporating a Bioluminescence-Fluorescence Dual Reporter and Streamlined CRISPR/Cas9 Functionality for Rapid in Vivo Localisation and Phenotyping. *PLoS Neglected Trop. Dis.* **2018**, *12*, No. e0006388.
- (59) daylight. <https://www.daylight.com/>.
- (60) Chemaxon. <http://www.chemaxon.com/>.
- (61) Openeye. <https://www.eyesopen.com/>.